Chapter -1

Nanomaterials – General Introduction

1.1. Preamble

Nanomaterials are the particles (crystalline or amorphous) of organic or inorganic materials having sizes in the range of 1-100 nm [1]. Nanomaterials are classified into nanostructured materials and nanophase/nanoparticle materials. The former refer to condensed bulk materials that are made of grains with grain sizes in the nanometer size range while the latter are usually the dispersive nanoparticles [2]. To distinguish nanomaterials from bulk, it is vitally important to demonstrate the unique properties of nanomaterials and their prospective impacts in science and technology.

Technology in the twenty first century requires the miniaturization of devices in to nanometer sizes while their ultimate performance is dramatically enhanced. This raises many issues regarding to new materials for achieving specific functionality and selectivity. Nanotechnology is the design, fabrication and application of nanostructures or nanomaterials and the fundamental understanding of the relationships between physical properties or phenomena and material dimensions. It is a new field or a new scientific domain. Nanotechnology also promises the possibility of creating nanostructures of metastable phases with non–conventional properties including superconductivity and magnetism. Another very important aspect of nanotechnology is the miniaturization of current and new instruments, sensors

and machines that will greatly impact the world we live in. Examples of possible miniaturization are computers with infinitely great power that compute algorithms to mimic human brains, biosensors that warn us at the early stage of the onset of disease and preferably at the molecular level and target specific drugs that automatically attack the diseased cells on site, nanorobots that can repair internal damage and remove chemical toxins in human bodies, nanoscaled electronics that constantly monitor our local environment.

Nanomaterials have properties that are significantly different and considerably improved relative to those of their coarser-grained counterparts. The property changes result from their small grain sizes, the large percentage of their atoms in large grain boundary environments and the interaction between the grains. Research on a variety of chemical, mechanical and physical properties is beginning to yield a glimmer of understanding of just how this interplay manifests itself in the properties of these new materials. In general, one can have nanoparticles of metals, semiconductors, dielectrics, magnetic materials, polymers or other organic compounds. Semiconductor heterostructures are usually referred to as one-dimensional artificially structured materials composed of layers of different phases/compositions. The semiconductor heterostructured material is the optimum candidate for fabricating electronic and photonic nanodevices [3].

It is seen that properties of these particles are quite sensitive to their sizes [4]. This is partly connected with the fact that surface to volume ratio changes with a change in particle size. A high percentage of surface atoms introduce many size-dependent phenomena. High surface area is an important feature of nanosized and nanoporous materials, which can be exploited in

many potential industrial applications, such as separation science and catalytic processing, because of the enhanced chemical reactivity [5, 6].

For optical applications, a wide range of nanostructure-based optical sources that include high performance lasers to general illumination can be fabricated. These industrial requirements can be accomplished by selecting an appropriate fabrication method of functional nanostructures with controlled size, shape and composition. However, assembling nanoparticles to form a nanostructure is a complex process. Numerous research groups are working out different synthetic strategies to find economically affordable ways for fabricating the nanostructures and simultaneously preserving the superior characteristics of the basic building units (nanoparticles) in various devices.

1.2. Classification of nanomaterials

Depending on the dimension in which the size effect on the resultant property becomes apparent, the nanomaterials can be classified as zero-dimensional (quantum dots) in which the movement of electrons is confined in all three dimensions, one-dimensional (quantum wires) in which the electrons can only move freely in the X-direction, two-dimensional (thin films) in which case the free electron can move in the X-Y plane, or three dimensional (nanostructured material built of nanoparticles as building blocks) in which the free electron can move in the X, Y and Z directions [7].

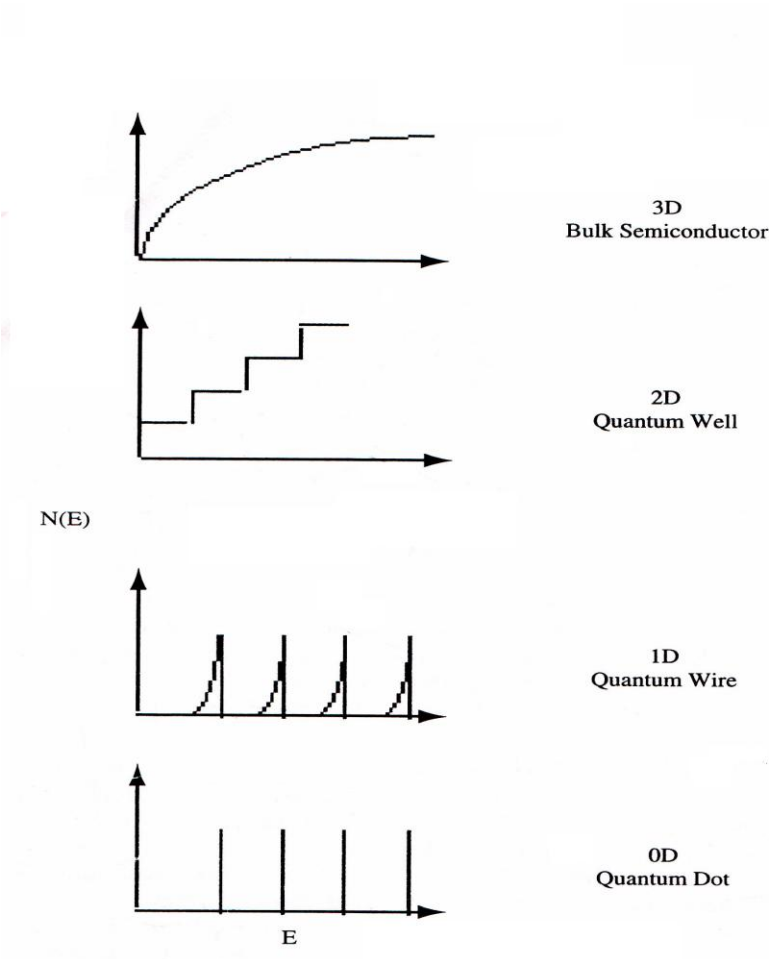

Figure 1.1 Variation of density of states with dimensionality

Semiconductor nanocrystals are zero-dimensional quantum dots, in which the spatial distributions of the excited electron-hole pairs are confined within a small volume, resulting in the enhanced non-linear optical properties. The density of states concentrates carriers in a certain energy range, which is likely to increase the gain for electro-optic signals. The quantum confinement of carriers converts the density of states to a set of discrete quantum levels. With consideration the small size of a semiconductor nanocrystal, its

electronic properties are significantly affected by the transport of the single electron, giving the possibility of producing single electron devices [8]. The schematic diagram in figure1.1 illustrates the variation of density of states with dimensionality.

Passing from three dimensions to two dimensions the density N(E) of states changes from a continuous dependence $N(E) \sim E^{1/2}$ to a step like dependence. The optical absorption edge for a quantum well is at a higher photon energy than for the bulk semiconductor and, above the absorption edge, the spectrum is stepped rather than smooth the steps corresponding to allowed transitions between valence-band states and conduction-band states, while, at each step, sharp peaks appear corresponding to electron-hole (exciton) pair states.

In the case of zero dimensional systems, the density of states is illustrated as a delta function. The low-dimensional structure has proven to be very promising for application to semiconductor lasers, which is mainly due to the quantum confinement of the carriers and the variation of the density of states with dimensionality [9]. The density of states has a more peaked structure with the decrease of the dimensionality. This leads to a reduction of threshold current density and a reduction of the temperature dependence of the threshold current.

Nanomaterials and related devices can be classified into three major categories, and suitable preparative methods are identified depending on the desired resultant structures [10]. The first category of nanomaterials consists of isolated, substrate-supported or embedded nanoparticles, which can be synthesized by physical vapor deposition (PVD), chemical vapor deposition (CVD), inert gas condensation, aerosol processing, precipitation from supersaturated vapors, liquids, or solids etc. Low–dimensional semiconductor

structures are usually fabricated by highly sophisticated growth techniques like molecular beam epitaxy (MBE) and metallorganic chemical vapor deposition (MOCVD). Quantum dots can be grown in a relatively easy way *via* the chemical methods including the colloidal method, sol-gel method, self assembly, embedding in polymers, encapsulation in zeolites or in glasses and so forth. Many terms have been used to describe these ultra small particles, such as quantum dots, Q-particles, clusters, nanoparticles, nanocrystals and others. Usually the zero-dimensional structures prepared in physical methods like MBE and MOCVD are called quantum dots by physicists while the small particles formed in chemical methods are called nanoparticles, nanoclusters, Q-particles or nanocrystallites by chemists [11].

The second category refers to materials having a thin nanometer-sized surface layer, which can be processed by techniques such as PVD, CVD, ion implantation, or laser ablation. The major advantage of these techniques is that the processing parameters can be suitably tuned to obtain a nanometer-sized surface layer. The self-organization and chemical self-assembly are also emerging as very important techniques for the deposition of materials layer-by- layer with controlled particle size and composition [12, 13]. Three-dimensional (3D) materials having nanometer sized grains belong to the third category. The crucial aspect related to the processing of these materials is control of the chemical composition and the grain size. For example, the metastable 3D nanostructures such as glass, gels, supersaturated solid solutions, or implanted materials can be prepared by quenching the high-temperature at equilibrium to the room temperature. The quenching helps to freeze the disordered structure with the composition varying on an atomic scale. Nanostructured-glass ceramics, which belong to the category of metastable 3D nanostructures, have been studied with immense interest in

recent years because of the potential engineering applications [14]. Another type of materials that belongs to this group is 3D ordered solid having building blocks as nanocrystals [15]. The microstructures of such solids comprise crystals with varying orientations separated by interfaces, which may be coherent, semi coherent or incoherent. The ideal preparative route for such structures would involve the optimization of the processing conditions to ensure the formation of a microstructure with controlled grain growth so that all the unique properties of the nanobuilding blocks are preserved.

1.3. Types of nanomaterials

1.3.1. Fractals

Real fractals are self-similar structures that result from physical, chemical or biological growth processes. A colloidal suspension is a fluid containing small charged particles, monomers, which are kept afloat by Brownian motion and kept apart by coulomb repulsion. Changing the chemical composition of the solution can induce a change in the interaction and an aggregation process can be initiated. Lin et al. [16] has indicated that the colloidal aggregation has universal features, which are independent of the nature of the colloidal systems. There are two limiting regimes for the colloidal aggregation. (1) A fast diffusion limited colloidal aggregation (DLCA) regime in which the reaction rate is determined solely by the time needed for the clusters to encounter each other by diffusion. (2) A slow reaction limited colloidal aggregation (RLCA) regime in which the cluster-cluster repulsion has to be overcome by thermal activation, a process that may require numerous encounters. The universal features have been demonstrated for colloidal aggregates of gold, silica and polystyrene [17, 18].

1.3.2. Porous materials.

Porous materials are characterized by a solid network having voids throughout the material and have been recognized as an important class of materials that can find applications in various fields [19, 20]. The percentage of porosity varies from ~ 5% to 25% in nanophase materials. The value is higher for consolidated oxide nanoparticles compared to the metal nanoparticles. The porosity enhances diffusion in nanophase ceramics. Doping of oxide nanomaterials with various types of dopants enables tuning of the properties to fit in a variety of applications. This has been a major area of research in recent years.

According to international union of pure and applied chemistry (IUPAC) porous materials are characterized by pore size categorized by sorption behaviour. They are microporous materials with pore sizes smaller than 2 nm, mesoporous materials with pores between 2 nm and 50 nm, and macroporous materials with pores larger than 50 nm [21].

Mesoporous materials can be synthesized by a wide range of techniques such as chemical etching, sol-gel processing and template assisted techniques. Ordered self assembly of hollow structures of silica, zeolites, carbon and titania has drawn much attention recently because of their applications in low loss dielectrics, catalysis, filtering and photonics [22,23]. The low density of the material results in very low dielectric constant, a candidate for low loss electronic devices. The synthesis of mesoporous materials can be useful for environmental cleaning and energy storage [24, 25].

1.3.3. Zeolites

Zeolites are often referred to as molecular sieves because their physical shapes allow them to sift materials. In structure they look like nanoscopic galleries or chambers interconnected by nanoscopic tunnels or pores, all dug out of a solid oxide. There are hundreds of different zeolite structures. The special nanopore structure of zeolites is the secret of their catalytic capabilities, and they represent highly profitable applications of nanotechnology [26, 27].

1.3.4. Fullerenes

Research in C_{60} fullerene has sparked a great effort in carbon related nanomaterials. Fullerene and carbon nanotubes can be chemically functionalized and they can serve as the sites/cells for nanochemical reaction. Carbon nanotubes have been known since the ingenious discovery of Iijima in 1991[28]. The long, smooth and uniform cylindrical structure of the nanotube is ideal for probe tips in scanning tunneling microscopy and atomic force microscopy. The ballistic quantum conductance of carbon nanotube was observed in defect free carbon nanotubes. This effect may have great impact on molecular electronics in which carbon nanotubes could be used as interconnects for molecular devices with no heat dissipation, high mechanical strength and flexibility [29-33].

Self-organisation and chemical self-assembly are promising techniques that provide inexpensive routes for the fabrication of nanostructures [34, 35]. In the immediate future, one can expect the miniaturization revolution in device fabrication to reach its peak in various industries. However, a recent study predicts that there is an optimum limit for miniaturization beyond which the second law of thermodynamics no longer holds [36].

1.3.5. Self assembly passivated nanocrystals superlattices

Self-assembly passivated nanocrystals superlattices involve self-organization into monolayers, thin films, and superlattices of size selected nanoclusters encapsulated in protective compact organic coating. A key step in this process is the fabrication of size and shape controlled nanocrystal assemblies that have the potential to assemble into large superlattice crystals for technological applications [37].

Size and even shape-selected nanocrystals behave like a molecular matter and are ideal building blocks for two and three-dimensional cluster self-assembled superlattice structures [38-40]. The electric, optical, transport and magnetic properties of the structures depend not only on the characteristics of individual nanocrystals, but also on the coupling and interaction among the nanocrystals arranged with long-range translational and even orientation order [41]. Self-assembled arrays involve self-organization into monolayers, thin films and superlattices of size-selected nanocrystals.

1.3.6. Micelles

When the surfactant concentration exceeds the critical micelle concentration (cmc) in water, micelles are formed as aggregates of surfactant molecules. In normal micelles the hydrophobic hydrocarbon chains of the surfactants are oriented toward the interior of the micelle, and hydrophilic groups of the surfactants are in contact with the surrounding aqueous medium. Above the cmc the physical state of the surfactant molecules changes dramatically, and an additional surfactant exists as aggregates or micelles. The bulk properties of the surfactant change around the cmc, such as osmotic pressure, turbidity, surface tension, conductivity and self-diffusion.

Reverse micelles are formed in the nonaqueous medium where the hydrophilic head-groups are directed toward the core of the micelles and the

hydrophobic groups are directed outward. In the case of reverse micelles there is no obvious cmc because the number of aggregates is usually small and they are not sensitive to the surfactant concentration. The general method of using reverse micelles to synthesize nanoparticles can be divided into two cases. The first case involves the mixing of two reverse micelles. Due to coalescence of the reverse micelles, exchange of the materials in the water droplets occurs, which causes a reaction between the cores and the nanoparticles are formed in the reversed micelles. The second case involves mixing one reactant that is solubilised in the reversed micelles with another reactant that is dissolved in water. Metal nanoparticles can be prepared by reducing metal salts in the reversed micelles. Reducing agents such as $NaBH_4$, N_2H_4 and sometime hydrogen gas were used [42-45].

1.3.7. Self assembled monolayers

Self assembled monolayers (SAM) are a prototypical form of nanotechnology: the molecules that form the SAM carry the instructions required to generate an ordered, nanostructured material without external intervention. SAMs demonstrate that molecular-scale design, synthesis, and organization can generate macroscopic materials properties and functions. Although the details of the thermodynamics, kinetics and mechanisms of assembly will differ significantly, SAMs establish a model for developing general strategies to fabricate nanostructured materials from individual nanometer-scale components (molecules, colloids, or other objects). SAMs are important components of many other forms of nanotechnology. Because SAMs can assemble onto surfaces of any geometry or size, they provide a general and highly flexible method to tailor the interfaces between nanometer-scale structures and their environment with molecular precision. SAMs can control the wettability and electrostatic nature of the interfaces of individual

nanostructures and thus their ability to organize into large assemblies. SAMs add chemical functionality and thermodynamic stability to the surfaces of relatively simple inorganic nanostructures (quantum dots, superparamagnetic particles, nanowires) and make it possible to connect them to more complex systems [46].

1.3.8. NC core/shell structures

Methods for overcoating a semiconductor nanocrystal (NC) with a second semiconductor material are well developed, and different kinds of core/shell structures have been successfully constructed including CdSe/ZnS, CdSe/ZnSe, CdSe/CdS, FePt/Fe_3O_4, CdTe/CdSe and CdSe/ZnTe core/shell nanoparticles. There are some requirements to prepare core/shell systems by epitaxy growth: (a) The existing NC seeds must withstand the conditions under which the second phase is deposited, (b) The surface energies of the two phases must be sufficiently similar so that the barrier for heterogeneous nucleation of the second phase is lower than that for homogeneous nucleation and (c) the seed NC and the overcoat material must not readily interdiffuse under the deposition conditions. Metal oxide nanoparticles (e.g. Fe_3O_4, TiO_2, MnO, $BaTiO_3$ etc.) can also be produced using this method [47-51].

1.3.9. Nature's nanoparticle factories

There are also different cellular organisms creating and using nanoparticles. One can find Fe_3O_4, Fe_3S_4, CdS, La $(NO_3)_2$, HUO_2PO_4, Ag, Te, Se, Au and Tc nanoparticles in natural systems. The most amazing example is the creation and use of magnetite nanoparticles enabling the use of biomagnetism. The Fe_3O_4 crystals exhibit a magnetic moment and enable the organism to navigate within the magnetic field of earth. Magnetotactic bacteria live in anaerobic environments and the magnetic sensor enables them to swim downwards, away from the oxygen rich water-air surface [52, 53].

1.4. Properties of nanomaterials - size effect

Nanocrystals cover a size range that is intermediate to the molecular size regime on one hand and the macroscopic bulk on the other. The size-dependent catalytic properties of nanocrystals have been widely studied, while investigation on the shape (facet)-dependent catalytic behavior is cumbersome. It is seen that reactivity of nanoparticles increases with decrease in particle size, melting temperature of nanophases is considerably lower than their bulk counter parts and the color of a nanoparticle (especially semiconductors) changes with its size. At times a particle could behave as metallic or semi conducting depending on its size. The finite size of the particle confines the spatial distribution of the electrons, leading to the quantised energy levels due to size effect. This quantum confinement has application in semiconductors, optoelectronic and in non-linear optics [54-56].

1.4.1. Surface plasmon resonance

Colloidal solutions of spherical gold nanoparticles exhibit a deep red color due to the well-known surface plasmon absorption. The surface plasmon resonance is caused by the coherent motion of the conduction band electrons, which interacts with an electromagnetic field. The observed color originates from the strong absorption of the metal nanoparticles when the frequency of the electromagnetic field becomes resonant with the coherent electron motion. The frequency and width of the surface plasmon absorption depends on the size and shape of metal nanoparticles as well as on the dielectric constant of the metal itself and the surrounding medium. Noble metals such as copper, silver and gold, have a strong visible light plasmon resonance, whereas most other transition metals show only a broad and poorly resolved absorption band in the ultraviolet region [57, 58].

The various interesting properties exhibited by oxide nanoparticles are the consequences of the size reduction. The enhancement in electrical conductivity is predicted for nanosized conducting ceramics as a result of space charge contribution from the interfaces [59]. Size effects play a crucial role in influencing the domain dependent magnetic and dielectric characteristics.

Another interesting effect is size quantization in semiconducting nanoparticles [60]. As the sizes of the semiconductor nanoparticles are reduced to dimensions (<5 nm) comparable to an exciton diameter, the energy gap between the valence and the conduction band increases. Consequently, the optical absorption shows a blue shift [61].

Reduction in particle size also enhances self-diffusion, solute diffusion and solute solubility in nanomaterials. Enhanced diffusivity and solubility can be attributed to defective atomic coordination at the grain boundaries in the nanocrystals [62]. The higher fraction of the grain boundaries in nanocrystals also results in higher values of specific heat compared to conventional polycrystals [63].

The large surface-to-volume ratio of nanocrystals greatly changes the role played by surface atoms in determining their thermodynamic properties. The reduced coordination number of the surface atoms greatly increases the surface energy so that atom diffusion occurs at relatively lower temperatures [64]. Nanocrystals usually have faceted shape and mainly enclosed by low index crystallographic planes. The density of surface atoms changes significantly for different crystallographic planes, possibly leading to different thermodynamic properties.

It is known that mechanical properties of a solid depend strongly on the density of dislocations, interface-to-volume ratio and grain size. A

decrease in grain size significantly affects the yield strength and hardness. The grain boundary structure, boundary angle, boundary sliding and movement of dislocations are important factors that determine the mechanical properties of the nanostructured materials. One of the most important applications of nanostructured materials is in superplasticity, the capacity of a polycrystalline material to undergo extensive tensile deformation without necking or fracture. Grain boundary diffusion and sliding are the two key requirements for super-plasticity [65].

The improved ductility of a brittle ceramic oxide when prepared in nanocrystalline form is worth noting. The enhanced interdiffusion among the grains in nanocrystals helps the grain boundaries slide by one another, thereby improving the ductility [66].

1.4.2. Magnetic properties

Magnetic materials exhibit size-dependent magnetic properties that range from ferromagnetic to paramagnetic to super paramagnetic with decreasing size. The magnetic properties of nanoparticles differ from those of bulk mainly in two points. The large surface-to-volume ratio results in a different local environment for the surface atoms in their magnetic coupling/interaction with the neighboring atoms, leading to the mixed volume and surface magnetic characteristics. Unlike bulk ferromagnetic materials, which usually form multiple magnetic domains, several ferromagnetic particles could consist of only a single magnetic domain. In the case of a single particle being a single domain, the superparamagnetism occurs, in which the magnetization of the particles are randomly distributed and they are aligned only under an applied magnetic field and the alignment disappears once the external field is withdrawn. In ultra-compact information storage the size of the domain determines the limit of storage density [67, 68]. Magnetic

nanocrystals have other important applications such as in color imaging [69], bioprocessing [70], magnetic refrigeration [71] and Ferro fluids [72]. Similarly, the properties (e.g. Meissner effect) of superconductors also depend on particle size. To understand the physicochemical and optoelectronic properties of nanoparticles and to exploit them for commercial applications, it is important to have dependable techniques for determining the sizes and shapes of nanoparticles. The giant magneto resistance (GMR) and colossal magneto resistance (CMR) materials offer exciting possibilities for magnetic sensors, magneto resistive read heads and magnetoresistive random access memory [73].

1.4.3. Mechanical properties

Grains are crystallized domains that combine to form a larger polycrystalline particle. As the grain size approaches the particle size, we have single crystal nanoparticles. Except for a single-crystal nanoparticle, in which the grain size and particle size are identical, the nanoparticles have randomly oriented grains. The atomic planes within a grain can be directly imaged using high-resolution transmission electron microscopy (HRTEM) [74]. The higher density of the consolidated nanophase material as compared to the theoretical density (74%) of powder compact may be attributed to the filling up of the pores by the enhanced diffusion, which arises out of an extrusion-like deformation in the consolidated nanophase. This process has been experimentally verified by the STM and atomic force microscopy (AFM) studies on metal nanoparticles [75]. The grains of the consolidated nanophase materials do not exhibit any preferred orientations in contrast to the micrograined samples. The random orientations of the grains in nanophase suppress the dislocation motion in these materials. In order to account for the unique properties of nanomaterials, it is imperative to understand the interface

characteristics, perhaps on an atomic scale. In nanomaterials, the randomly oriented crystals have incoherent interfaces where the atoms are far from being in a perfect order, as in a lattice. The misfit among the crystals also results in the modification of the grain boundary atomic structure by reducing the atomic density and altering the coordination numbers of the atoms. The characterization of the iron-containing nanomaterials by Mossbauer spectroscopy revealed the grain boundary structures of these materials with defective coordination environments compared to a perfect lattice [76]. The defective coordination environments also make the atoms at the interface more reactive.

The parameter, strain, may also govern the stability of the finely divided particles, as it has been found that the presence of large number of interfaces in a nanomaterial leads to the generation of intrinsic strain in nanosized particles [77]. Apart from the intrinsic strain, the method of preparation may induce an extrinsic strain in these materials. The line broadening obtained by X-ray diffraction helps to estimate the strain present in the sample [78].

The increase in oxygen permeability through the nanophase material can be attributed to the highly defective surfaces of the metal oxide nanoparticles, which eventually provides easy pathways for the oxygen diffusion. It has been experimentally verified that the defects such as dislocations are rare in nanoparticles [79-81]. The reason for the lack of dislocations in nanophase materials can be attributed to the image forces in the finite atomic ensembles that pull the dislocations, which also affects the mechanical properties of nanoparticles [82].

1.5. Synthesis routes

The drive for finding novel routes for the synthesis of nanomaterials has gained considerable momentum in recent years, owing to the ever-increasing demand for smaller particle sizes. Prior to the synthesis of a nanophase material, the size and the dimensional features of the material to be prepared have to be defined. Accordingly a suitable preparative method can be adopted. Controlling the microstructures at the atomic level has been of great multidisciplinary interest to fields such as physics, chemistry, material science and biology. As the particle size is scaled down to a few nanometers, the constituting atoms exhibit highly defective coordination environments. Most of the atoms have unsatisfied valences and reside at the surface. In short, microstructural features such as small grain size, large number of interfaces and grain boundary junctions, pores and various lattice defects that result from the chosen routes for the synthesis, contribute significantly to the unique physical and chemical properties of nanomaterials [61, 83, 84].

The top-down approach of preparing nanoparticles involves breaking of bulk particles to nanosizes (e.g. ball milling) and the bottom–up approach involves atom-atom or molecule-molecule assembling of nanoparticle micelle. Nucleation and growth are the two important processes in the bottom-up approach. Nucleation is a process in which an aggregate of atoms is formed and is the first step of the phase transformation. The growth of nuclei results in the formation of large crystalline particles. Therefore, study of nanocrystals and its size-dependent structures and properties is a key in understanding the nucleation and growth of crystals. An important area of nanotechnology concerns the development of reliable processes and techniques for synthesis and characterization of nanoparticles over a range of sizes and shapes.

Typical nanoparticles are agglomerates of several primary particles. The agglomerates are termed as secondary particle. The secondary particle size is obtained by scanning electron microscopy, where as the X-ray line broadening helps to estimate the primary particle size or crystallite size. Minimizing the agglomeration and driving the properties exclusive to the primary particles are the important objectives in the synthesis of nanoparticles [3].

The major issues for the synthesis of nanoparticles are (i) the control of the particle size and composition, and (ii) the control of the interfaces and the distribution of the nanobuilding blocks within the fully formed nanostructured materials. The synthesis routes for nanomaterials are broadly classified to three categories like soft chemical solution routes, solid-state reaction methods and gas phase condensation methods. In this work we have adopted the soft chemical synthesis routes.

1.5.1. Soft chemical solution routes

Within the last few decades, advances in solid-state chemistry have resulted in substantial progress towards a better understanding of the solid state, and have even led to the development of some predictive capabilities in crystal chemistry. Nonetheless, in more recent years, entirely new ways of thinking have appeared. The term “soft chemistry” or “chimie douce” is often applied in a general manner to refer to these new routes, these new ways of thinking.

The concept of “chimie douce” or “soft chemistry” was introduced by French solid-state chemists, Livage and Rouxel, which is widely accepted by the scientific community [85, 86]. Tailarable and controllable chemical reactions in the solution, which are soft and weak, could obtain the required composition and structures with suitable shapes without high temperature

treatment and grinding or powder processing. The softness and weakness route overcomes the traditional “hard and hot” approach and makes the synthesis of compounds feasible. The soft chemistry technique has shown a remarkable success in preparation of colloidal clusters with controlled size and shapes. Soft chemistry is classified as sol-gel processing, ion exchange and condensation, intercalation-deintercalation, pillaring–grafting processing, colloids-emulsification etc. The field of soft chemistry is not restricted to a well-defined area of science. While sol-gel processes represent one essential component of soft chemistry, other reactions dealing with intercalation-deintercalation, pillaring-grafting, and exchange-condensation are no less important. The unifying theme behind these various processes is a common scientific approach, similar methods of characterization, and analogous problematics related to metastability and phase transitions. Perhaps the term "soft chemistry" should be regarded more as a way of thinking, a new paradigm in solid-state chemistry. In all cases the precursor compounds play a significant role because the structural mosaic (or block) of the resulting compounds must be contained in the precursors and the structural evolution of the precursor must be in the desired manner. Soft chemistry can be defined as the processing of exclusively non-hazardous substances without waste products or by-products except those that can be completely recycled.

1.5.1.1. Sol-gel (colloidal) processing

Sol-gel (colloidal) processing is a popular processing route for the synthesis of a wide variety of materials in desired shapes (particles, fibers, or films). The formation of a sol by dissolving the metal alkoxide, metal-organic, or metal-inorganic salt precursors in a suitable solvent is the primary step in a sol-gel process. Upon drying the sol, a polymeric network is formed in which

the solvent molecules are trapped inside a solid (gel). Subsequent drying of the gel followed by the calcinations and sintering leads to the final ceramic product. As the reacting species are homogenized at the atomic level in a sol-gel process, the diffusion distances are considerably reduced compared to a conventional solid-state reaction, thereby the product forms at much lower temperatures. Depending on the nature of the precursor, which can be an aqueous solution of an inorganic salt or metal-organic compound, the species involved in the intermediate steps of the sol-gel process differ. The nature and composition of the intermediate species formed depend on the oxidation state, the pH, or the concentration of the solution [87, 88].

1.5.1.2. Chemical precipitation

The kinetics of nucleation and particle growth in homogeneous solutions can be adjusted by the controlled release of the anions and cations. Careful control of the kinetics of the precipitation can result in monodispersed nanoparticles. Once the solution reaches a critical supersaturation of the species forming particles only one burst of nuclei occurs. Thus it is essential to control the factors that determine the precipitation process, such as the pH and the concentration of the reactants and ions. Organic molecules are used to control the release of the reactants and ions in the solution during the precipitation process. The particle size is influenced by the reactant concentration, pH and temperature. By controlling these factors, nanoparticles with narrow size distributions such as $Zr(OH)_4$, $BaTiO_3$, CdS, HgTe, CdTe have been produced.

Although the method of using precipitation to prepare nanoparticles is very straight forward and simple, very complicated nanostructures can also be

constructed using this method such as CdS/HgS/CdS, CdS/$(HgS)_2$/CdS and HgTe/CdS quantum well systems and other core/shell structures [89-94].

1.5.1.3. Solvothermal/hydrothermal synthesis

Solvothermal/Hydrothermal Synthesis involves the exploitation of the properties of water (solvent) under high pressure and temperature for the preparation of fine powders of advanced ceramic oxides. The advantage of the hydrothermal method over the other solution routes is that the final product readily forms at a low temperature without calcinations. Fine crystallites of the desired phase with excellent composition, morphology control, powder reactivity and purity can be obtained. The precursor sol is prepared from oxides, hydroxides, nitrates or halides of the corresponding metallic elements and subjected to hydrothermal synthesis, which is carried out in a high-pressure apparatus or hydrothermal bomb (autoclave) [95, 96]. Various other techniques can be combined with the hydrothermal technique to form a kind of hybrid technique for the synthesis of nanoparticles. Examples of such techniques are hydrothermal-sonochemical and hydrothermal-microwave processing [97, 98].

1.5.1.4. Solvent process

The solvent process utilizes solvable salts or compounds that can be dissolved by acids as the raw materials: they can then mix in water or other solvents to be uniform solutions. Then the solvents are evaporated by heating evaporation, spraying dryness, flaming dryness, or cooling dryness. Finally the heat decomposition reactions result in the nanoparticles or nanocomposites. Besides the solvent evaporation method, the emulsion techniques, such as partial microemulsion, double microemulsion, pressure homogenization-emulsification or modified spontaneous emulsification solvent diffusion methods can be categorized as solvent methods [99, 100].

1.5.1.5. Microemulsion synthesis

Among the various techniques, the microemulsion-mediated synthesis has been particularly of interest to size selective preparation and self-assembly of nanoparticles because of the excellent control on the particle size that can be achieved through appropriate surface modification of the micelle. Microemulsion can be defined as an isotropic, thermodynamic stable system constituting the micrometer-sized droplets (micelle) dispersed in an immiscible solvent and an amphiphilic surfactant species on the surface of the micelle. The crucial aspect of the microemulsion route is the control of the nanoparticle size through suitable selection and addition of a surfactant prior to the hydrolysis of the metal alkoxide sol (reverse micelle or water-in-oil emulsion). The addition of the surfactant molecules creates aqueous domains (nanoreactors) in the range of 0.5-10 nm. By properly tuning the water/surfactant ratio, which is critical in deciding the final particle size, the diameter of the aqueous droplets can be tuned.

The method has been recognized as the most appropriate for the synthesis of ultra-fine magnetic nanoparticles for potential applications in magnetic recording media, biomedical, and related fields [101-103].

1.5.1.6. Polymerization

Polymerization is a very common method for preparation of nanomaterials. During polymerization the formation of microemulsion is a very much important factor, which has been the focus of extensive research worldwide due to its importance in a variety of technological applications. These applications include enhanced oil recovery, combustion, cosmetics, pharmaceuticals, agriculture, metal cutting, lubrication, food, enzymatic catalysis, organic and bio-organic reactions, chemical synthesis of nanoparticles and nanocapsules etc. Nanocapsules consisting of an inorganic

core and a polymer shell offer interesting prospects in various applications [104].

1.5.1.7. Latex process

The latex process utilizes two different solvents that are not soluble each other to form a uniform and homogeneous microemulsion with the help of surfactant and dispersions. Microemulsion is usually a transparent and isotropic thermodynamic system composed of surfactants, dispersions (polymers, alcohols), oil (hydrocarbons) and water (or electrolytical water solutions). Polymer dispersions made of a variety of monomers, including styrene, butyl acrylate and methyl methacrylate, surround the latex droplet. The solid phase could be from the emulsion, so that the processes of nucleation, growth, assembly, aggregation, etc. could be limited inside a micro/nanoemulsion droplet to form the micro/nanospheres which avoids further aggregation of the nanoparticles [105-107].

1.5.1.8. Oxidation processes

The oxidation process oxidises and deoxidizes directly the raw materials in the liquid phase or quasi-liquid phase state. The oxidation phases can be used to prepare the nanoparticles of metals, alloys or oxides, in either water solutions or organic solutions [108, 109].

1.5.1.9. Microwave plasma processing

Microwave plasma processing has emerged as a major processing route for oxide ceramics. The method is attractive because the kinetic and thermodynamic barriers that are usually encountered in conventional solid-state synthesis can be overcome with short processing time. The faster reaction rate may be attributed to the reverse heating profile during the exposure of reactants to microwaves as compared to the conventional furnace heating. The compound forms when energy transfer occurs between the electrons and the

other species in the plasma. The parameters that decide the energy transfer between the electrons and the neutral or ionized species in the plasma are the frequency of the source and the number of collisions made. The precursor solution is introduced into the microwave cavity through a nozzle. Both aqueous and non-aqueous solutions are used for the synthesis of oxide powders. The aqueous precursor solution is usually a nitrate solution containing the metal ions of the desired phase. Water being highly polar, absorbs the microwaves quickly and evaporates from the precursor solution. The residual material upon further exposure to the plasma reacts with the oxygen species in the plasma to form fine metal oxide particles. The technique has been used for the preparation of some model binary oxides zirconia (ZrO_2), alumina (Al_2O_3) or solid solution between them [110,111].

1.5.1.10. Electric dispersion reaction

Electric dispersion reaction is a precipitation reaction that is carried out in the presence of a pulsed electric field to synthesize ultra fine precursor powders of advanced ceramic materials. The technique involves subjecting the reactor liquid (metal-alkoxide solution) to a dc electric field (3 to 10 kV/cm at pulsing frequencies in the range 1 to 3 kHz). Under the applied electric field, the sol is shattered to micron-sized droplets, termed as microreactors, which contain hydrous precursor precipitate. The formed precursor powders can be thermally processed to obtain oxide nanoparticles [112].

1.5.1.11. Pyrolysis

Pyrolysis is a chemical process in which chemical precursors decompose under suitable thermal treatment into one solid compound and unwanted waste evaporates away. Upon completion, the desired new substance is obtained. Generally, the pyrolytic synthesis of compounds leads to powders with a wide size distribution in the micrometer regime. To get a

uniform nanosized material, some modifications or revisions of the pyrolytic preparation procedure and reaction conditions are needed such as slowing of the reaction rate or decomposition of the precursor in the inert solvent. MCO_3, MC_2O_4, MC_2O_2, $M(CO)_x$, MNO_3, glycolate, citrate and alkoxides are the common precursors that are used. Poly vinyl alcohol (PVA) and Poly ethelene glycol (PEG) are commonly used as protecting agents. Pyrolysis can be used to prepare different kinds of nanoparticles including metals, metal oxides, semiconductors and composite materials [113-116].

1.5.1.12. Spray pyrolysis

As an alternative method to sophisticated processing routes with the potential for commercial scale-up, spray pyrolysis has been widely used for the synthesis of ultrafine particles and thin films. The precursor solution (sol), which contains the metal ions dissolved in the desired stoichiometry, is sprayed through a nozzle and suspended in gaseous atmosphere (aerosol generator). The suspended droplets are thermally processed to the product phase by allowing the sol droplets to drift through the heated zone of a furnace. Spray pyrolysis has many variations based on the differences in thermal processing step. Some of them are aerosol decomposition, evaporative decomposition, spray roasting, and spray calcinations [117, 118].

1.5.2. Solid state reaction methods

Solid-state reactions offer the possibility of generating nanoparticles by controlled phase transformations or reactions of solid materials. The advantage is its simple production route. The solid-state reaction technique is a convenient, inexpensive and effective preparation method of mono-disperse oxide nanoparticles in high yield. Nanooxides were successfully synthesized by solid-state reactions at ambient temperature [119, 120].

1.5.2.1. Evaporation

Evaporation in gases is a method that evaporates metals, alloys or ceramics so that the atoms bump each other and also atoms of inert gases or they react with active gases. Condensation in the cold gases results in the formation of nanoparticles and nanocapsules. Heating by a resistance heater or a high frequency induction furnace is the simplest method in laboratories for evaporating the metals. The resistance heater can be made of graphite, tungsten wire or other kinds of metal wires. In the earliest experiments metals were put in a tungsten basket inside a vacuum chamber and then evaporated in argon atmosphere of 1-50 Torr. The metal smoke deposited on the water-cooled inner wall of the chamber. The crystallographic properties of various nanoparticles such as Mg, Al, Cr, Mn, Fe, Co, Ni, Cu, Zn, Ag, Cd, Sn, Au, Pb and Bi were investigated systematically by TEM observations [121-124].

1.5.2.2. Arc discharge/plasma

The formation mechanism of nanoparticles in plasma is that matter clusters with high activity exist in the plasma, which could exchange rapidly the energy with the reacted matter clusters, beneficial to the reaction between them. When the reacted matter clusters leave the high temperature in the flame tail region of the plasma, the rapid decrease of the temperature lets the clusters be in the saturation state in dynamic equilibrium thus they are dissociated. The rapid cooling/quenching leads to the nucleation of crystallites and the formation of nanoparticles/nanocapsules. According to the method of production the plasma can be of two kinds: direct current arc plasma and high frequency plasma. Direct current arc plasma uses the direct current arc in inert/active gases to ionize the gases, generate the high temperature plasma and melt the materials. The cooling, reaction and condensation of the evaporating matters lead to the formation of nanoparticles and nanocapsules.

The arc vaporization/discharge method has been widely used for the formation of fullerenes and related materials [125].

1.5.2.3. Laser/electron beam heating

Electron beam heating has been used in the fields of melting, welding, sputtering and micro manufacturing. The electrons emit from the cathode of the electron gun where the temperature is very high due to the application of the high voltage that is necessary for the emission of electrons. Thus the high vacuum must be kept in the electron gun.

Actually the electron gun inside the TEM can be conveniently used for electron beam heating and irradiating of the materials. Another efficient method is the laser heating, which has several advantages like (i) the heating source is outside the evaporation system, (ii) any materials, including metals, compounds, ceramics, etc., can be evaporated and (iii) there is no contamination from the heating source. Both the methods are efficient for evaporation of materials with high melting points. The method was developed for formation of carbon nanotubes, carbon nanocapsules, and carbon nanoparticles in which polyyne-containing carbons were heated and irradiated by an electron beam in a TEM [126, 127].

1.5.2.4. Mechanochemical synthesis

The drive for low cost commercial production of nanophased materials has led to the development of a mechanical milling process, which involves continuous milling of the reactive powders over a period of time. The apparatus used for milling should have the following features: generating high energy through high impact velocity and frequency during the milling process to enhance the reaction rate and the productivity, and easy scale-up of the mill capacity. The reactive components after prolonged milling undergo reduction in size and increase in surface area, which leads to the enhanced diffusion of

the reactants. Hence, the product phase crystallizes at much lower temperatures compared to conventional solid-state synthesis [128, 129].

1.5.2.5. Congealing

Rapidly cooled materials are often unstable as a result of changes in their physical properties due to imperfect crystallization. In the process of congealing melted material is atomized into droplets that are very quickly solidified. This increases the possibility of the material crystallizing in different metastable forms [130, 131].

1.5.2.6. Combustion synthesis

In combustion synthesis, there is the exploitation of an excess heat-generating or exothermic reaction, to overcome the activation energy barrier for the formation of products. The precursor is a redox mixture that contains an organic compound (fuel) as the reducing agent and a metal salt as the oxidizing agent. When heated to ignition point of the fuel the mixture instantaneously burns to form the product. Large volumes of gas produced during the process also help the precursor particles to disintegrate to smaller particles. The major advantage of the method is that it is fast, requiring the least external energy input and gives high output with the possibility of producing wide variety of ceramic oxides [132, 133].

1.5.2.7. Laser ablation and related methods

Recently researchers have developed a laser ablation technique to synthesize nanoparticles of controlled particle sizes and compositions. The technique involves the vaporization of a target using pulsed laser, which is then followed by the controlled condensation in a diffusion cloud chamber under well-defined conditions of temperature and pressure. A wide variety of

metal oxides, carbides and nitrides can be synthesized in nanoscale dimensions using this method [134, 135].

1.5.3. Gas phase condensation methods

The production of nanoparticles by condensation of gaseous precursor molecules comes under the category of aerosol processes [136, 137]. For the synthesis of nanoparticles or ultrafine particles the gas phase condensation is a suitable method. The initial step in this process is the formation of gaseous precursor molecules by a suitable physical or chemical method in aerosol reactors [138]. The precursor molecule then reacts in the vapor phase to form tiny nucleus of the desired phase. The size of a typical nucleus thus formed has dimensions comparable to that of a molecule of a refractory oxide. Subsequently the primary particles undergo collision and coalescence to form aggregates, which in turn form agglomerates held together by the weak van der Waal's forces [139].

1.5.3.1. Flame processing

Oxide nanoparticles are produced commercially on a large scale in a flame reactor. The precursor in vapour phase is fed into a reactor in the presence of oxygen and ignited. The burning step may also take place in other gaseous atmospheres such as inert gas, hydrogen, or methane [140]. The method is commercially used for the production of industrially useful silica (SiO_2) from silicon tetrachloride vapour. Al_2O_3 from $AlCl_3$ and TiO_2 from $TiCl_4$ are also prepared by this method.

1.5.4. Sonochemical processing

Application of ultrasound in chemical synthesis has initiated a new fascinating field in processing technology. As the name suggests the sound wave act as the energy source when the respective sol of the material to be prepared, is exposed to high intensity ultrasound (50 –500 W/cm^2). The

underlying mechanism of sonochemical processing route consists of the formation, growth, and collapse of the bubbles of the sol upon exposure to acoustic waves to form the product phase. The collapse of the bubbles leads to very high temperature (~ 5273 K), high pressure (1.01325 x 10^8 Pa)**,** high heating and cooling rate (10^{10} K/s), and short-lived transient species. The extreme conditions during acoustic cavitation enable the reactants to cross the activation energy barrier in a very short amount of time to form the product phase. The magnetite Fe_3O_4 is useful as a magnetic ferrofluid in applications such as data storage. In order to prepare fine-grained magnetite particles, an efficient alternative to high-energy milling is the use of sonochemical preparation from volatile organometallic precursors [141, 142].

1.5.5. Reduction methods

There are various reduction methods used to synthesize transition metal nanoparticles in colloidal solution, such as reduction with alcohols, hydrogen gas, sodium borohydride, hydrazine and sodium citrate. Methods like thermal reduction, photochemical reduction, sonochemical reduction, ligand displacement of organometallics, metal vapor condensation, and electrochemical reduction are also in use for the synthesis of metal nanoparticles [143-156].

1.5.6. Catalytic methods

1.5.6.1. Homogeneous catalysis

In homogeneous catalysis, transition metal nanoparticles dispersed in an organic or aqueous solution or in a solvent mixture are used as catalysts. The colloidal nanoparticles must be stabilized to prevent their aggregation. However it was shown that the better the capping, which makes the nanoparticles stable in solution, the lower the catalytic activity becomes because the active surface sites are better protected.

Some common stabilizers used to cap transition metal nanoparticles in colloidal solution include polymers, block copolymers, dendrimers, surfactants and other ligands [157-160].

1.5.6.2. Heterogeneous catalysis

In heterogeneous catalysis, transition metal nanoparticles are supported on various substrates and used as catalysts. There are three major ways by which heterogeneous transition metal nanocatalysts are prepared; adsorption of the nanoparticles on to supports, grafting of nanoparticles on to supports and fabrication of nanostructures on to supports by lithographic techniques. Some common supports that have been used in the preparation of supported transition metal nanoparticles include carbon, silica, alumina, titanium dioxide, grafting onto polymeric supports, and lithographic fabrication on supports [161-164].

1.5.7. Physico-chemical methods of preparation of thin films

1.5.7. 1. Sputtering

Sputtering is a convenient method for preparing films. By sputtering, different elementary materials are ionized or heated to form the plasma before depositing on substrates. Sputtering can be employed for preparing the nanoparticles embedded in the thin films, or so called granular films. High voltage current is applied between the cathode and the anode in atmosphere of inert and active gases leads to glow discharge. The ions during the process of discharge bump the target that serves as the cathode, so that the atoms of the target materials could evaporate from the surface. The cooling and the condensation in inert gases and/or the reaction in active gases of the evaporated atoms result in the formation of nanoparticles and nanocapsules or thin films. This method has many advantages. No crucible is needed, particles of metals with a high melting point can be prepared, the evaporation surface

can be large, particles of alloys can be synthesized using active gases, granular thin films can be prepared, the narrow size distribution of the particles can be controlled well and nanocomposite materials can be produced if several different materials are used as targets. The voltage, current, gas pressure, and target are the most important factors, which affect the formation of nanoparticles [165, 166].

1.5.7.2. Pan coating

Pan coating is a technique using polymer or different mixtures of polymers as film coating agents. The method can be based on the simultaneous spraying of aqueous solutions of a film-forming polymer and an appropriate cross linking agent. Cross-linking of the polymer is achieved *in-situ* in the film during the coating of the pellets in a fluidized bed [167].

1.5.7.3. Spray-drying

Spray drying is the process of spraying a solution into a warm drying medium to produce nearly spherical powder granules that are relatively homogeneous. There are four stages in the spray drying. They are (i) rotary atomization of the liquid feed to generate a fine spray (ii) injection of the hot gas stream into the radially distributed spray (iii) rapid vaporization of the solvent to yield the powder product (iv) centrifugal separation of the spherical particles from the gas stream [168].

1.5.7.4. Successive ionic layer adsorption and reaction (SILAR) method

One of the newest solution methods for the deposition of thin film is SILAR method, which is also known as modified form of chemical bath deposition [169].

1.5.7.5. Chemical vapour deposition (CVD)

In CVD the vapourised precursors are introduced into a CVD reactor and adsorb onto a substance held at an elevated temperature. These adsorbed molecules will either thermally decompose or react with other gases/vapors to form crystals. The CVD process consists of three steps: (a) mass transport of reactants to the growth surface through a boundary layer by diffusion (b) chemical reactions on the growth surface, and (c) removal of the gas-phase reaction byproducts from the growth surface. Catalysts, usually transition metal particles such as Fe, Ni, and Co are used in the CVD process. Strained-induced Stranski-Krastanow is used to produce nanoparticles in the CVD process [170-172].

1.5.7.6. Physical vapour deposition (PVD)

PVD involves condensation from the vapor phase. The PVD process is composed of three main steps: (a) generating a vapor phase by evaporation or sublimation of the material, (b) transporting the material from the source to the substrate, and (c) formation of the particle and/or film by nucleation and growth. Different techniques have been used to evaporate the source such as electron beam, thermal energy, sputtering, Cathodic arc plasma, and pulsed laser. Si nanowire, GeO_2 nanowire, Ga_2O_3 nanowire, ZnO nanorod, GaO nanobelt and nanosheet, SnO_2 nanowire, nanoribbon, nanotube, etc., have been synthesized using PVD [173-177].

1.5.7.7. Coacervation-phase separation

Coacervation-phase separation is a method to use a coacervation-inducing agent to reach the coacervation-phase seperation during/after the solvent evaporation to form the microcapsules or the nanocapsules. The coating can be controlled by changing the parameters during the process, so

that the drug content, particle size distribution, biomedical properties etc. of the microcapsules/nanocapsules can be controlled [178, 179].

1.5.7.8. Air suspension

Air suspension is a common technique to utilize fluidized bed systems for selecting the particle materials, which can be developed for coating the nanoparticles to realizing the micro/nanoencapsulation of drug products and food particles [180].

1.6. Characterization techniques

Several techniques such as X-ray diffraction (XRD), Transmission electron microscopy (TEM), Scanning electron microscopy (SEM), Scanning tunneling microscopy (STM), Atomic force microscopy (AFM), Dynamic light scattering (DLS), Small angle X-ray scattering (SAXS) and Small angle neutron scattering (SANS) have been extensively used for determining the sizes and shapes of nanoparticles and is not surprising that all these techniques have their merits and demerits [64].

1.6.1. X-ray diffraction

The powder XRD is the most common and first hand instrument used by solid-state scientists. X-ray diffraction is a powerful method to investigate the detailed structure, composition and related properties of nano-materials. This information can be derived from peak position, intensity and the peak profile. A great advantage of X-ray powder diffraction is that it requires virtually no sample preparation, in comparison to other techniques. The sample can be either in the form of smear or compact flat pack or a capillary and is exposed to monochromatic beam of X-ray and the diffracted beam intensity is collected in a range of angles (2θ) with respect to the incident beam. The intensity corresponding to a constructive interference of the

diffracted beam from a crystallographic plane is observed as peak, corresponding to the Bragg angle (θ). In all other angles a background is obtained. The intensity corresponding to background has several origins [181].

Although microscopic methods provide a direct visualization of nanocrystals, the images alone provide a misleading view. Unreacted molecular species as well as small amorphous particles are difficult to see using microscopic techniques, yet they can comprise a large fraction of nanocrystalline particles. For such samples, X-ray diffraction studies help to determine the extent of crystallanity and are useful to differentiate between crystalline and amorphous nanomaterials. The intense and well-defined peaks show strong reflections from various crystal planes. The positions of the peaks provide an accurate fingerprint of the crystal structure of the nanocrystals. Such an unambiguous determination of nanocrystals structure is especially important, as many nanocrystalline materials adopt metastable crystal structures distinct from the bulk solid [182].

A powder diffraction pattern contains information on phases present (peak positions), phase concentrations (peak heights), structure, degree of crystallanity or amorphous content (background hump) and crystallite size/strain (peak widths/broadening). The width of the peaks in a particular phase pattern provides an indication of the average crystallite size. Large crystallites give rise to sharp peaks, while the peak width increases as crystallite size reduces. Crystallite size does not equal the size of the particle, as one particle can be a conglomerate of several crystallites. Peak broadening also occurs as a result of variation in d-spacing caused by microstrain. The breadth of the peaks in an X-ray diffractogram provides a way to determine the average crystallite size, assuming no lattice strain or defects, through the Debye-Scherrer formula.

$$t = 0.9\lambda/\beta\cos\theta \qquad (1.1)$$

where t is the thickness of the crystal, λ is the wavelength of the X-rays, β is the full width at half maximum of the diffraction peak, and θ is the Bragg angle of the peak [182, 183].

Good agreement between the nanocrystal sizes are usually found from XRD and TEM measurements. Extensive analysis and simulations of the XRD patterns of nanocrystals can provide information on nanocrystal defect density and type as well as the presence and distribution of strain in the nanocrystal lattice.

Rietveld analysis is used to obtain information about the structural parameters of the phases present. Detailed structural information, like space group, characteristic interplanar spacings, lattice parameters, atomic site coordinate, atomic occupation, etc. can be derived for the phases in the materials [184].

Information about nanoparticle crystallanity can be obtained by comparison of the average particle sizes estimated by powder XRD and TEM methods. The width of the XRD reflexes provides information about the X-ray coherence length, which is close to the average size of the single crystalline domain inside the nanocrystal, where as TEM images show the total size of a nanoparticle. Particle sizes estimated by these methods are referred to as "XRD-size" and "TEM-size" respectively [185].

1.6.2 Transmission electron microscopy (TEM)

The transmission electron microscope (TEM) has emerged as a very powerful tool for probing the structure of nanophased materials. It can give morphological information of shape and size of phases in a microstructure. It can reveal the nature of crystallographic defects. A detailed study of both line defects and plane defects can be carried out in TEM. Structural information

can be obtained from the TEM directly as well as indirectly. Indirect structural information is obtained by making use of the various diffraction techniques available in the TEM. Direct information about structure is obtained by high-resolution electron microscopy (HREM). TEM is capable of yielding composition analysis at nano level. The crystalline lattice serves as a grating to lead to the diffraction of the electrons. With the TEM essentially all incoming electrons are transmitted through a specimen that is suitably thin. Rather than being absorbed, electrons may be scattered (i.e. deflected in their path) by the atoms of the specimen. The fast electrons used in a TEM are capable of penetrating many atomic planes and so are diffracted by crystalline regions of material just like X-rays. Their wavelength (~ 0.04 nm for E_o ~ 100 keV) is much less than a typical atomic-plane spacing (~ 0.3 nm) so that according to the Bragg equation $n\lambda = 2d\sin\theta$, Bragg angles θ are small. In addition the integer n is usually taken as unity, since n^{th} order diffraction from planes of spacing d can be regarded as first order diffraction from planes of spacing d/n [64].

Diffraction represents elastic scattering of electrons in a crystal. The regularity of the spacing of these nuclei results in a redistribution of the angular distribution of the scattered intensity. Instead of continuous distribution over scattering angle, there are sharp peaks centered around certain scattering angles, each twice the corresponding Bragg angle θ. In the TEM this angular distribution can be displayed by magnifying the diffraction pattern first formed at the back focal plane of the objective lens. Examination of the TEM image of the polycrystalline specimen shows that there is a variation of electron intensity within each crystallite. This diffraction contrast arises either from atomic defects within the crystal or the crystalline nature of the material itself, combined with the wave nature of transmitted electrons.

The resolution of the TEM could be improved by special arrangements of the magnetic fields serving as focuses of the electron beam, by enhancing the energy of the electrons. The main advantage of the HREM are the direct observations of the detailed nanostructures, such as the core/shell structure, the interfaces and the surfaces, the atomic defects (including point defects, dislocation, planar defects) the twin structures etc [64, 183].

The nanocrystal characterization can be done using transmission microscopy. Here, an electron beam is used to image a thin sample in transmission mode. The resolution is a sensitive function of the beam voltage and electron optics: a low-resolution microscope operating at 100 kV might have a 2-3 Å resolution while a high voltage machine designed for imaging can have a resolution approaching 1 Å. Since nanocrystalline samples range from ten to hundreds of angstroms in size, this type of microscopy allows both the interior crystal structure and the overall particle shape to be measured.

A single TEM picture of a nanocrystalline sample can provide an enormous amount of information. Low resolution TEM can also be used to determine sample distributions and shapes. Higher resolution images show the discrete nature of the crystalline interior of nanoparticles and can detect the presence of certain crystalline defects; the Fourier transform of such images provides a measure of the lattice spacing and crystallographic parameters.

More sophisticated analysis of high-resolution TEM images can provide even deeper insight into subtle structural aspects of nanocrystals. Simulation of high-resolution images can, in principle, provide data concerning whether the average bond length in a nanocrystals is uniform or variable within the nanocrystals interior. Another exciting prospect is the use of TEM to provide direct information about nanocrystals surfaces including reconstructions and dynamic motions of atoms at surfaces. Thus the TEM

picture gives information about the particle shape, size and size distribution. At least 1000 particles should be counted. The size distribution in the measured range can be plotted in the form of a histogram [186-188].

1.6.3 Scanning electron microscopy (SEM)

Scanning electron microscope (SEM) is an instrument, which is used to observe the morphology of a sample at higher magnification, higher resolution and depth of focus compared to an optical microscope. Herein, an accelerated beam of mono-energetic electrons is focused on to the surface of the sample and is scanned over it on a small area. Several signals are generated and appropriate ones are collected depending on the mode of its operation. The signal is amplified and made to form a synchronous image on a cathode ray tube, the contrast resulting from the morphological changes and variation of atomic number over the area probed. A camera is used to photograph the image or it may be digitized and processed on a computer. The characteristic X-rays emitted may be analyzed for their energy and intensity (EDX), the energy being the signature of the element emitting them and the intensity as to how much of it is present. SEM while having lower resolution than TEM, is able to image nanoparticles on bulk surfaces and for direct visualization of nanocrystals in larger assemblies [183, 189, 190].

1.6.4. Scanning probe microscopy (SPM)

The most recent developments in determining the surface structure are the atomic force microscope (AFM) and scanning tunnelling microscope (STM). These techniques are capable of imaging the local surface topography with atomic resolution [191].

1.6.4.1. Atomic force microscopy (AFM)

Atomic force microscope (AFM) or scanning force microscope (SFM) is the most generally applicable member of the SPM family, which is the key tool in nanotechnology research and development. It is based on minute but detectable forces between a sharp tip and atoms in the surface. In 1986, Gerd Binning invented the atomic force microscope (AFM). The tip is mounted on a flexible arm called cantilever, and is positioned at subnanometer distance from the surface. When the tip is brought close to a sample surface the interatomic forces between them causes the cantilever to bend and this motion is detected optically by a laser beam which is reflected off the back of the cantilever. If the tip is scanned over the sample surface then the deflection of the cantilever can be recorded as an image, which in its simplest form, represents the three dimensional shape of the sample surface. If the sample is scanned under the tip in the X-Y plane, it feels the attractive or repulsive force from the surface atoms and hence it is deflected in the Z direction [192].

Atomic force microscopy can be applied in two ways viz., contact mode and non-contact mode or tapping mode**.** In the contact mode, the tip is within a few angstroms from the surface, and the interaction is between the individual atoms at the tip and on the surface. The description of atomic force interaction in the contact mode is highly complex. It requires a molecular dynamics stimulation of the coulombic interaction between charges or charge distribution, polarization due to induced dipole moments and quantum mechanical forces when electron orbital starts to interact, for each pair of atoms from the tip and the surface. The contact mode is the usual choice to study surface morphology with atomic resolution [193].

In non-contact mode, the distance between the tip and the sample is much larger, between 2 and 30 nm. In this case one describes the forces in terms of the macroscopic interaction between bodies. In the tapping mode, the sample should have a flat surface and the tip should be a spherical particle. Several forces may play a role *viz* electrostatic force, in the case of potential difference between the tip and the sample, and magnetostatic force, if the sample is magnetic. Forces in the non-contact mode are typically 2-4 orders of magnitude smaller than in the contact mode. In this mode, details on the sub nanometer scale are not obtained because the interaction is now between larger portions of the tip and the sample. The non-contact mode is of particular interest for imaging magnetic domains or electronic devices.

Atomic force microscope is used to identify a sample's atomic level surface characteristics, including its magnetic and electrical properties and the topography. An AFM creates a highly magnified three-dimensional image of a surface. With the AFM it is possible to directly view features on a surface having a few nanometer-sized dimensions including single atoms and molecules on a surface. This gives scientists and engineers an ability to directly visualize nanometer sized objects and to measure the dimensions of the surface features [194].

1.6.4.2. Scanning tunneling microscopy (STM)

Scanning tunneling microscope is one of the key tools in nanotechnology, which belongs to the SPM family. Scanning tunneling microscope was invented by Gerd Binning and Heinrich Rohrer in 1982. Scanning tunneling microscopy is used to study the properties of surfaces at the atomic level. The basic principle of STM is based on the tunneling current between the metallic tip, which is sharpened to a single atom point and a

conducting material. A small bias voltage is applied between an atomically sharp tip and the sample. If the distance between the tip and the sample is large, no current flow. However when the tip is brought very close, without physical contact, a current flows across the gap, between the tip and the sample. Such current is called tunneling current which is the result of the overlapping wave functions between the tip atom and the surface atom. In the presence of small bias voltage, the electrons can travel across the vacuum barrier separating the tip and sample in the presence of small bias voltage. The magnitude of the tunneling current is extremely sensitive to the gap distance between the tip and the sample, the local density of electronic states of the sample and the local barrier height. With the help of STM, atomic information of the surface can be mapped out. Scanning tunneling microscopy (STM) measures the topography of surface electronic states using a tunneling current that is dependent on the separation between the probe tip and a sample surface. It is typically performed on conductive and semiconductive surfaces. A common application consists of atomic resolution imaging, electrochemical STM, Scanning tunneling spectroscopy (STS) and low current imaging of poorly conductive samples [64, 191, 194, 195-197].

1.7. Material studies

1.7.1 Vibrating sample magnetometer (VSM)

Magnetic properties of a material could be measured by various types of facilities, among which a vibrating sample magnetometer (VSM) is one of the most commonly used tools [198, 199]. A VSM is a magnetometer based on the mechanism of electromagnetic induction. A sample is vibrated in the vicinity of a set of pick up coils. The flux change caused by the moving magnetic sample causes an induction voltage across the terminals of the pick

up coils that is proportional to the magnetization of the sample. The VSMs have a comparatively high sensitivity for measuring the magnetic moment ($5x10^{-5} – 2x10^{-9}$ Am^2) [200].

1.7.2. FTIR spectroscopy

In vibrational spectroscopy we look at the changes in vibrational motion of atoms in a molecule, which are greatly influenced by the masses of atoms, their geometrical arrangement and strength of their chemical bonds. Both IR and Raman spectra involve IR radiation and results from transition between quantized vibrational states and provide a complementary image of molecular vibrations. The two spectroscopic techniques differ in their instrumentation and the way light quanta interact with the molecules. Thus interaction of IR radiation with vibrating molecule is only possible if the molecular dipole moment is modulated by the vibration (IR active) while a molecular vibration is only observable in the Raman spectrum if there is modulation of molecular polarizablity by the vibration (Raman active) [183].

IR encompasses a spectral region from red end of visible spectrum (12500 cm^{-1}) to the microwave (10 cm^{-1}) region in the electromagnetic spectrum and is conveniently divided into near IR (12500 to 4000 cm^{-1}), mid IR (4000 to 400 cm^{-1}) and far IR (400 to 10 cm^{-1}). The main significance of this division is that most fundamental molecular vibrations occur in mid-IR making this region richest in chemical information while overtones and combination of fundamental vibrations especially those involving hydrogen atoms appear in the near IR and far IR contains vibrations involving heavy atoms, lattice modes of solids and some rotational absorption of small molecules. Fourier transform spectrometers are superior to the dispersive IR spectrometers. FTIR spectrometers are based upon Michelson interferometer. The powder sample is mixed with nujol to form a thick paste and held between

salt plates or thoroughly mixed with potassium bromide (KBr) and pressed using a hydraulic press to form pellets and then placed in the sample holder of the instrument [201].

1.7.3. UV-visible spectroscopy

Ultraviolet and visible spectroscopy is a reliable and accurate analytical method that allows for the analysis of a substance. Specifically, ultraviolet and visible spectroscopy measures the absorption, transmission and emission of ultraviolet and visible light wavelengths by matter [202, 203].

The UV-visible spectroscopy is used to study molecules and inorganic ions in solution as well as in the solid state. Although there are distinct regions of the electromagnetic spectrum, the ultraviolet and visible region of the electromagnetic spectrum are linked in UV-visible spectroscopy because the similarities between the two regions allow many of the research techniques and tools to be used for both region. Many molecules absorb ultraviolet or visible light which are lower in energy than cosmic, gamma or X-rays and higher in energy, than infrared, microwave and radio waves. The wavelength that is absorbed depends on the chemical composition [204]. The intensity of the band is directly proportional to the concentration of an absorbing group or molecule. UV-visible spectroscopy enables the characterization of functional groups in a molecule as well as the determination of their concentration as per Beer-Lamberts law. When ultraviolet or visible light strike atoms or molecules they can either bounce off or cause electron to jump between energy levels. Absorption of ultraviolet or visible light electromagnetic radiation causes electron to move from lower energy levels to higher energy levels. Above a certain energy or frequency known as the absorption edge, intense absorption occurs. In electronically insulating ionic solids, the absorption edge may

occur in the UV, but in photoconducting and semiconducting materials, it may occur in the visible or near IR region [205].

1.7.4. Luminescence

Luminescence is the name generally given to the emission of light by a material as a consequence of absorbing energy. Graphs showing the dependence of luminescence power on the wavelength, frequency or energy of radiation quanta are called luminescence spectra. Photoluminescence (PL) uses photons or often UV light for excitation. The dependence of photoluminescence power on the frequency or wave length of the exciting light with its constant intensity at all frequencies is referred to as the excitation spectrum In cathodoluminescence (CL), cathode rays or high-energy electrons are the means of excitation. Themoluminescence (TL) in solids is the light emission that takes place during heating of a solid following an earlier absorption of energy from radiation [206]. Two types of photoluminescence may be distinguished. For a short time lapse of $\leq 10^{-8}$ sec between excitation and emission, the process is known as fluorescence. Since the energy transitions does not involve a change in electron spin fluorescence effectively ceases as soon as the excitation source is removed. For much longer decay times the process is known as phosphorescence. This involves a change in electron spin and may continue long after the removal of the source of excitation [183].

Absorption of a photon places an atom or molecule in a naturally metastable excited state. This metastable state ultimately re-emits the energy in one or more of three possible relaxation pathways. The first is radiative, *via* either fluorescence or phosphorescence. The second pathway is nonradiative processes such as internal conversion or energy transfer. Internal conversion is

the process where rotational-vibrational energy is lost to the surroundings as the molecule cascades down the rotational-vibrational ladder. The third possibility is chemical change, such as breaking bonds to form a new chemical species [207].

Luminescent emission involves optical transitions between electronic states characteristic of the particular material. Luminescence may also involve impurities or structural defects, in which case electronic states involved in the luminescence can be approximated in terms of band states of the perfect crystal perturbed by the impurity. In semiconductors the external excitation generates excess electron hole pairs. The process by which excess carriers recombine can be classified as radiative and non-radiative. In the former, excess energy is emitted, either wholly or partially as radiation. Such processes lead to luminescence. In the latter case excess energy is dissipated ultimately as heat by various mechanisms [208].

Optical excitation of semiconductor nanoparticles leads to band edge and deep trap luminescence. The emission of radiations in semiconductors arises out of the basic process of radiative recombination of electrons and holes. The energy of the emitted photons is equal to the energy difference between those of electrons and holes. These carriers can have different energies depending upon whether they are free or bound. At very low temperature due to carrier-freeze out the electrons and holes are bound to various impurities and defects. As the temperature is increased these carriers are released at a rate depending on the activation energies**.** As particles become smaller, the surface/volume ratio and hence the number of surface states increases rapidly reducing the excitonic (bound electron-hole pair) emission. Thus surface states often determine the physical properties, especially the optical properties, of nanoparticles [209-211].

Nanoparticles may have an increased natural radiative rate and thus enhanced quantum efficiency due to the effects of quantum confinement on the electron- phonon coupling and density of states (DOS). The important contribution to non radiative rate is trapping to surface states [212].

Passivation of surface states is a key requirement in increasing the luminescence efficiencies of nanoparticles relative to bulk materials [213].

1.7.5. Photocatalysis

The mechanism of the photocatalysis involves adsorbing the pollutant molecules, from air or water, on the surface of semiconducting particles, which are then excited using the ultraviolet or visible radiation of the appropriate energy to generate electron (e^-) and hole (h^+) pairs within the particle volume. These e^-/h^+ pairs then migrate to the particle surface and serve as redox sites for the destruction of the surface-adsorbed pollutants [214].

Heterogeneous semiconductors in the field of photocatalysis were investigated deeply because of its high efficiency, commercial availability and high chemical stability. When the semiconductor particles are illuminated with UV-visible light, an electron promotes from the valence band to the conduction band due to photoexcitation, thus leaving an electron deficiency or hole in the valence band; in this way, electron/hole pairs are generated. These electron hole pairs can either recombine or can interact separately with other molecules. Both reductive and oxidative processes can occur at/or near the surface of the photoexcited semiconductor particle. In aerated aqueous suspensions, oxygen adsorbed on the surface of the catalyst acts as an electron trap on the conduction band and electron/hole recombination can be effectively prevented and lifetime of holes is prolonged [215, 216].

The photocatalytic activity of a semiconductor has been known to be dependent on the various material parameters, which include the average nanocrystallite size, powder morphology, specific surface area, crystallanity, and phases involved [217, 218]. Surface area and surface defects play an important role in the photocatalytic activities of metal oxide. The reason is that, doping of metal oxide with metal and/or transition metals increases the surface defects [219]. Although wide band gap semiconductors such as TiO_2 and ZnO have been investigated extensively, they are in general not photocatalytic when excited by visible light, which is a basic requirement for efficient solar energy utilization. Therefore, other oxide materials capable of photoinduced charge separation upon excitation in the visible spectral region have gained new interest. An example is $BiVO_4$, which exhibits good catalytic activity in photooxidations [220-223].

The newly synthesized ZnO:Mn^{2+} has been observed as an excellent photocatalyst under visible illumination. ZnO:Mn^{2+} photocatalysts showed promising results for degradation of organic dye with visible light irradiation when used as suspended colloids. The development of such photocatalysts may be considered a breakthrough inlarge-scale utilization of heterogeneous photocatalysis *via* visible light to address water contamination and environmental pollution. Here, we assumed that upon illumination with visible light, ZnO:Mn^{2+} generates electron–hole pair at the tail states of conduction band and valence band, respectively. The generated electron transfers to the adsorbed methylene blue (MB) molecule on the particle surface because it is a cationic dye. The excited electron from the photocatalyst conduction band enters into the molecular structure of MB and disrupts its conjugated system, which then leads to the complete decomposition of MB. Hole at the valence band generates OH• via reaction with water or OH−, might be used for

oxidation of other organic compounds. Being a cationic dye MB acquires electron from excited donor states and decomposes [224].

Photoelectrochemical water splitting using semiconductor photocatalysts has been considered as an attractive route to convert solar energy directly into hydrogen (solar hydrogen) for future renewable energy applications [225-228]. The efficient utilization of the visible portion of the solar spectrum is essential to both solar hydrogen generation and the photocatalytic decomposition of organic pollutants. Bismuth vanadate ($BiVO_4$) has been recognized as a visible-light-driven photocatalyst for these applications [229-233].

1.7.6 Thermal analysis

Thermal analysis deals with the action of heat on the physical properties of the materials. Various attempts have been made to understand the effect of applying heat in order to manipulate the properties of materials. Some of the specific properties that can be studied using thermal analysis are mass, enthalpy, heat capacity and co-efficient of thermal expansion and thermal conductivity [234].

Thermogravimetric analysis (TGA) automatically records the change in weight of a sample as a function of either temperature or time. The sample usually a few milligrams are taken in the pan of the thermogravimetric apparatus and heated at a constant rate of 1 to 20 $^{o}Cmin^{-1}$. The sample shows weight changes during a thermal event like decomposition. The decomposition temperature and the temperature during the completion of the thermal event depend mainly on heating rate, nature of solid and atmosphere above the sample.

Differential thermal analysis (DTA) measures the difference in temperature between a sample and an inert reference material as a function of

temperature during a programmed change of temperature. The temperature of the sample and reference should be the same until some thermal event such as melting, decomposition or change in crystal structure occurs in the sample. The sample temperature either lags behind (for endothermic change) or leads (for exothermic change) the reference temperature depending on the nature of the thermal event. The temperature difference is detected by the net voltage of the thermocouple arrangement attached to the sample and reference pans and the difference in temperature ΔT is plotted against the temperature to get the DTA curve [183, 235].

Differential Scanning Calorimetry (DSC) is a thermal analysis technique very similar to differential thermal analysis used for quantitative measurement of enthalpy changes. Instead of allowing a temperature difference to develop between the sample and the reference material, DSC measures the energy that has to be supplied to keep the temperature the same. ΔE is plotted against the temperature to get the DSC curve [236-238].

1.7.7 Dielectric properties at low frequencies (~1 to 13 MHz)

Dielectric properties may be defined by the behaviour of the material in a parallel plate capacitor. The ac conductivity has been calculated from the measurements of capacitance and dielectric loss. The dielectric constant (ε) is calculated from the measured capacitance (C) using the relation

$$\varepsilon = 11.3\ CL/A \qquad (1.2)$$

then ac conductivity is given by the relation

$$\sigma_{ac} = 2\pi\ \varepsilon_o\ \varepsilon \tan\delta \qquad (1.3)$$

where L is the thickness, A the area of cross-section of the electrode on the sample, tan δ is the dielectric loss tangent and ε_o is the permittivity of free space [239].

1.7.8. Dielectric properties at microwave frequencies

The dielectric parameters can be calculated knowing the volumes of the sample and the cavity resonator [240]. The basic principle involved in the technique is that the field within the cavity resonator is perturbed by the introduction of the dielectric sample through the non-radiating slot. The resonant frequency and the quality factor of the cavity get shifted due to perturbation [241].

Theory

When a material is introduced into a resonant cavity, the cavity field distribution and resonant frequency are changed which depend on geometry, electromagnetic properties and its position in the fields of the cavity. Dielectric material interacts only with the electric field in the cavity. According to the theory of cavity perturbation, the complex frequency shift is related as

$$\varepsilon_r' - 1 = \frac{f_0 - f_s}{2f_s}\left[\frac{V_c}{V_s}\right] \tag{1.4}$$

$$\varepsilon_r'' = \frac{V_0}{4V_s}\left[\frac{Q_0 - Q_s}{Q_0 Q_s}\right] \tag{1.5}$$

the relative complex permittivity of the sample is given by,

$$\varepsilon_r^* = \varepsilon_r'' - j\varepsilon_r' \tag{1.6}$$

the effective conductivity, $\sigma_e = 2\pi f_s \varepsilon_o \varepsilon_r''$ (1.7)

dielectric loss tangent, $\text{Tan}\,\delta = \varepsilon_r''/\varepsilon_r'$ (1.8)

where ε_r' is the real part of the relative complex permittivity, which is known as dielectric constant and ε_r'' is the imaginary part of the relative complex

permittivity associated with the dielectric loss of the material. V_s and V_c are the volumes of the sample and the cavity resonator respectively and ε_o is the permittivity of free space [242-244].

1.7.9. Magnetic properties at microwave frequencies

Theory

When a small sample is introduced in to the cavity resonator, it causes frequency shift. The real and imaginary parts of the complex frequency shifts are given by

$$\mu'_r = 1 + \left[\frac{\left(\lambda^2_g + 4a^2\right)}{8a^2}\right]\left[\frac{\left(f_0 - f_s\right)}{f_s}\right]\frac{v_c}{v_s} \qquad (1.9)$$

μ_r' is the real part of complex permeability, λ_g is the guided wave length, f_0 and f_s are the resonance frequency of the cavity loaded with empty capillary tube and capillary tube containing the sample [245- 247].

$$\mu''_r = \left[\frac{\left(\lambda^2_g + 4a^2\right)}{16a^2}\right]\frac{v_c}{v_s}\left[\frac{1}{Q_s} - \frac{1}{Q_0}\right] \qquad (1.10)$$

μ_r'' is the imaginary part of complex permeability , Q_s and Q_0 are the quality factors of the cavity, loaded with capillary tube containing the sample and empty capillary tube.

$$\text{The guided wavelength, } \lambda_g = \frac{2d}{n} \qquad (1.11)$$

Where n = 1, 2, 3, …….

$$\text{Magnetic loss tangent Tan } \delta = \mu_r''/\mu_r' \qquad (1.12)$$

1.7.10. BET surface area analysis

Brunauer, Emmett and Teller (BET) method is used to measure total surface area of the nanosized materials [248]. In this technique, the amount of nitrogen adsorbed at constant temperature (200 °C) by a given weight of sample is measured using a Micromeritics, ASAP 2020 surface area analyzer. The volume of the nitrogen adsorbed in a monolayer V_m is calculated from the BET equation

$$\frac{P}{V_0(P_0 - P)} = \frac{1}{V_m C} + \frac{P(C-1)}{V_m C P_0} \qquad (1.13)$$

where P = Nitrogen pressure

P_0= Vapour pressure of nitrogen at the temperature of the liquid N_2 calculated at STP.

V_0 = Volume of nitrogen adsorbed at pressure P and temperature of the liquid N_2 calculated at STP.

C = Constant related to the difference between the heat of liquefaction of the adsorbate

A plot of $[\frac{P}{V_0(P_0 - P)}]$ against $\frac{P}{P_0}$ will give $\frac{C-1}{V_m C}$ as slope and $\frac{1}{V_m C}$ as intercept, from which V_m can be calculated. Knowing the value of V_m, surface area (S) can be calculated by using the equation

$$S = \frac{N_A V_m}{W \times 22414} \qquad (1.14)$$

where N = Avogadro number

A = Area occupied by one N_2 molecule (1.6×10^{-20} m^2)

V_m = Monolayer volume at STP

1.8. Applications

The nanoparticles could have many applications in biology and medicine, including protein purification, drug delivery and medical imaging [249]. The combination of nanotechnonology and molecular biology has developed into an emerging research area: nano-biotechnology. For *in vivo* biomedical applications, the purity, dispersity and stability of the multifunctional magnetic nanoparticles in a physiological environment are highly important [250].

Magnetic nanostructures can be used as drug delivery carriers. Polymers are used to coat magnetic nanoparticles and are encapsulated to form nanocapsules or micelles [251]. Because of the potential benefits of multimodal functionality in biomedical applications, researchers would like to design and fabricate multifunctional magnetic nanoparticles and could lead to new opportunities in nanomedicine [252]. A novel concept termed "nanoclinic" in medical diagnostics refers to exploitation of the unique properties of oxide nanoparticles for biomedical applications. A typical example of a nanoclinic is the iron oxide Fe_2O_3 nanoparticles encapsulated by silica shell, which can be used in contrast magnetic resonance in medical diagnosis [253]. γ- Fe_2O_3 hollow nanoparticles exhibit a strong MR signal attenuation effect. FePt@ Fe_2O_3 yolk-shell nanoparticles and Pt@ Fe_2O_3 yolk-shell nanoparticles also show strong MR relaxation enhancement [254]. The porphyrin-modified Fe_3O_4 nanoparticles can act as a multifunctional nanomedicine that combines photodynamic therapy (PDT) anticancer

treatment and noninvasive magnetic resonance (MR) imaging [255]. Clearly the design and optimization of such structures is a matter of medical nanotechnology and holds promise as a noninvasive approach for dealing with many growths, tumors and diseases.

Noble metal nanostructures are being utilized for biodiagnostics, biophysical studies and medical therapy [256]. For example, taking advantage of the strong localized surface plasmon resonance (LSPR) scattering of gold nanoparticles conjugated with specific targeting molecules allows the molecule-specific imaging and diagnosis of diseases such as cancer [257]. The strong Plasmon absorption and photothermal conversion of gold nanoparticles has been exploited in cancer therapy through the selective localized photothermal heating of cancer cells [258]. The LSPR frequency for gold, silver and copper lies in the visible region. [259, 260]. Since copper is easily oxidized, gold and silver nanostructures are most attractive for optical applications.

For nanorods or nanoshells, the LSPR can be tuned to the near-infrared region, making it possible to perform *in vivo* imaging and therapy [261]. In addition to being strong near-IR absorbers, nanoshells can be strong scatters of NIR light. This opens up the potential for diagnostic imaging of tumors for early detection. Compared with molecular contrast agents such as indocyanine green, nanoshells have far larger scattering cross sections and a tunable optical response over a wide wave length range [262].

Several useful applications in the study of subcellular process of fundamental importance in biology have highlighted the potential of quantum dots (QDs) in nanotechnology. Nanoluminescent tags are quantum dots often attached to proteins to allow them to penetrate cell walls. These quantum dots exhibit the nanoscale property that their colour is size dependant. They are

made out of bio-inert materials. These tags solve two major problems of the old organic dyes, toxicity and the ability to use more than one colour of tags at the same time with a single light source [263].

The magnetic nanoparticles can combine QDs to exhibit magnetic and fluorescent properties and opens an avenue for designing and synthesizing sophisticated and multifunctional nanostructures [264]. The combination of superparamagnetism and fluorescence at nanometer scale should help the biological applications of multifunctional nanomaterials. For example, the Fe_3O_4-CdSe heterodimer nanoparticles bear two attractive features with high quality, superparamagnetism and fluorescence which allow their intracellular movements to be controlled using magnetic force and to be monitored using fluorescent microscopes [265].

Neuro-electronic interfaces are new idea of constructing nanodevices that will permit computers to be joined and linked to the nervous system. The construction of a neuro-electronic interface simply requires the building of a molecular structure that will permit control and detection of nerve impulses by an external computer. This challenge is a combination of computational nanotechnology and bio nanotechnology [266]**.** Nanotechnology may enter clinical oncology. We can ultimately envision utilizing nanoparticles as nanovehicles to deliver therapeutics to sites of disease notoriously difficult to treat, that is, the brain. An almost intractable problem in oncology is the treatment of primary brain malignancies and multiple metastatic deposits within the brain. Choi *et al* [267] have developed a "Trojan Horse" strategy to deliver nanoshells to the hypoxic regions of solid tumors**.**

Protein engineering is one of the more mature areas of nanobiotechnology because we really know how to make large numbers of proteins. With the mapping of the human genome, the new fields of post-

genomic science and proteomics are now being devoted to understanding what proteins do and how their functions can be improved by synthetic structures, including entirely artificial proteins [268].

Sensors are structures that indicate the presence of particular molecules or biological structures, as well as the amounts that are present. In order to sense chemical/biological species, the nanoparticles are conjugated with recognition molecules, which specifically bind the target analyte, while appropriate surface capping is required to minimize nonspecific binding. The binding of the target molecule to the recognition molecules causes a plasmon band shift due to a local refractive index (RI) change, serving as an optical sensing tool [269]. It is well documented that nanostructured materials such as carbon nanotubes (CNTs) [270] and nanowires are suitable for sensing a number of different gases. A group of scientists from the states [271] have successfully manufactured a nanostructured materials sensor for ammonia gas which can be tuned to eliminate the interference of water vapour.

Smart structures are a new emerging materials system that combines contemporary materials science with information science. The smart system is composed of sensing, processing, actuating, feedback, self-diagnosing and self-recovering subsystems. Four of the most widely used smart materials nowadays are piezoelectric $Pb(Zr,Ti)O_3$, (PZT) magnetostrictive $(Tb,Dy)Fe_2$, electrostrictive $Pb(Mg,Nb)O_3$, and shape memory alloy NiTi [272].

Recently nanotechnology is very useful in the field of forensics where new techniques are able to provide either improved performance over existing materials or enable information to be gleaned from a crime scene that would not otherwise have been possible. The ideal fingerprint powder will stick to the residues left by the finger, which give rise to the characteristic patterns that everyone identifies as a finger print, but not stick to anything else. Many

common materials also stick to the background, making a clear identification difficult. Nanotechnology is being used to engineer particles to overcome this problem [273].

Soft chemistry has shown a great success in fabricating functional and nanophase materials. Functional materials are distinctly different from structural materials and their physical and chemical properties are sensitive to a change in the environment such as temperature, pressure, electric field, magnetic field, optical wavelength, adsorbed gas molecules and pH [274]. Functional materials utilize their native properties and functions to achieve intelligent action. Bio-functional magnetic nanoparticles exhibit two features, specific binding and targeting. Hence they find several applications as pathogen detection, protein purification [275, 276] and toxin decorporation [277]. Detection of bacteria at ultralow concentrations without time-consuming procedures is advantageous in clinical diagnosis and environmental monitoring. Vancomycin-conjugated FePt nanoparticles are used to detect bacteria at very low concentrations [278].

The field of nanocatalysis has undergone an exponential growth during the past two decades [279]. Nanosized cuprous oxide and colloidal nanoparticles of platinum group metals have attracted much interest because of their potential application in catalysis [280, 281]. Metal nanoparticles have attracted a great interest in scientific research and industrial applications as catalysts owing to their large surface-to- volume ratios and quantum-size effects [282, 283]. The bimetallic nanoparticles display much higher catalytic activity than the corresponding monometallic nanoparticles, especially at particular molecular ratios of both elements [284].

Nanoporous and nanostructured films provide a route to low dielectric constant materials that will enable future generations of powerful

microprocessors [285]. They are the only route to achieve materials with refractive indices <1.2, a key feature for the future development of photonic crystal devices [286,287], enhanced omni-directional reflectors [288] and enhanced anti-reflection coatings [289].

Present orthodoxy

With in the broad family of functional materials, metal oxides are particularly attractive. The discovery of high T_C superconductors focused worldwide scientific attention on the chemistry of metal oxides. The phenomenal range of electronic and magnetic properties exhibited by these oxides is noteworthy. We have oxides with metallic properties at one end of the range and oxides with highly insulating behaviour at the other end. There are also oxides that traverse both these regimes. If we list the most important discoveries in solid state and material science in the last two-three decades, it would include high temperature superconductors [290,291], fullerenes and related materials [292,293], mesoporous silica [294], colossal magnetoresistance [295] and functional materials for electronics and photonics [296]. Many of these deals with metal oxides, and it is exciting to witness the increasing importance gained by these materials. Layered copper oxides exhibiting high-T_C superconductivity readily spring to mind as a good example [297]. Another example is the finding that certain perovskite manganese oxides display dramatic changes in their specific resistivities when subjected to magnetic fields, opening up the new sub-field of colossal magnetoresistance [298]. In traditional electronics, for example LCR (inductance-capacitance-resistance) circuits, the Ls and the Cs are invariably metal oxides. Oxide materials find applications in the area of integrated semiconductor devices [299], dielectrics in dynamic random access memories

[300], ferroelectrics in non-volatile memories [301], and decoupling capacitors [302]. Oxides are also at the heart of many fuel cells [303] and secondary battery materials [304]. Magnetic oxide nanoparticles are used in magnetic drug delivery and in hyperthermic cancer therapy [253]. Large quantities of nanoparticulate oxide materials are expected to be consumed in the preparation of transparent sunscreens for topical applications [305].

Scope of the present investigation

For decades metal-oxides have been extensively investigated by solid-state chemists [306]. Recently metal-oxide nanoparticles like, ferrites, vanadates, phosphates and tungstates have been the subject of much interest because of their unusual magnetic, catalytic, optical, and electronic properties [307]. Most of these properties are due to particles of uniform size and shape distribution. However, to obtain metal oxides as nanoscale materials with well-defined size, shape and composition, traditional solid-state synthesis methods are unsuitable [308].

Literature survey reveals that, ferrimagnetic materials by the name ferrites have attracted the attention of chemists, physicists and technologists since they exhibit magnetic as well as semi-conducting properties and because of their broad applications in several technological fields including catalysis, permanent magnets, magnetic fluids, magnetic drug delivery, microwave devices and high-density information storage [309, 310]. For any particular application, the magnetic nanoparticles must possess specific properties. For example, data storage applications require particles with stable switchable magnetic states to represent bits of information, states not affected by temperature fluctuations. In bio-medical applications, the nanoparticles must exhibit superparamagnetic behavior at room temperature [311]. Their high

resistivity and low hysteresis loss makes them suitable to use in microwave applications and radio electronics [312,313]. The properties of ferrite particles are strongly dependent on their size. Among the family of ferrite materials, cobalt ferrite, the most commercially significant particulate recording material is a well-known hard magnetic material with high coercivity and moderate magnetization and used in videotape and high-density digital recording [314]. Magnetic copper ferrites have important technological applications including magnetic information storage and biological and micro-electromagnetic devices [315].

Nowadays vanadium oxides and their derivative compounds have attracted considerable interests due to their redox-activity and layered structures. Silver vanadium oxides are important materials, owing to their ionic properties and as a cathode material in lithium ion batteries [316]. The development of photo catalysts working under UV-visible region is an important theme nowadays. Silver vanadium oxide phases are mostly synthesized by solid-state reactions. But the soft chemistry routes, rather remains unexplored.

$BiVO_4$ has attracted attention as a ferroelastic and ion conductive material [317,318]. These properties strongly depend on the crystal form. $BiVO_4$ has three main crystal forms, the zircon structure with tetragonal system and scheelite structure with monoclinic and tetragonal systems [319]. The obtained crystal form of $BiVO_4$ depends on the preparation method. Some synthesis methods for $BiVO_4$ have been reported [320,321]. Scheelite type monoclinic $BiVO_4$ is usually obtained by solid state and melting reactions at high temperatures, while tetragonal $BiVO_4$ is prepared in aqueous media by the low-temperature process. Comparative studies on the photocatalytic activities of scheelite tetragonal and scheelite monoclinic $BiVO_4$ have been

reported [322-323]. However, the preparation method of monoclinic $BiVO_4$ by an aqueous process at room temperature has not been yet developed. It will be of interest if the preparation method controlling the crystal forms under mild conditions is developed.

Phosphate ceramics are getting attention due to their variety of applications in optical, electrical, prosthetics and structural fields as fluorescent materials, dielectric substances, dental cements, metal surface coatings, fuel cells, pigments, etc [324-326]. Studies on transition metal phosphates like zinc phosphate is important since they are used as inorganic and biomaterials finding applications as catalysts, ion exchangers and in low thermal expansion ceramic materials [327]. Synthetic micro porous and layered materials are of considerable interest for a wide variety of industrial and chemical applications. When used as hosts of impurity doped optical materials phosphates show better performance than silicates [328].

Zinc phosphate is a non-toxic white inorganic pigment featuring corrosion protection and adhesion capability and is the first bio-ceramic to be proposed in dental applications [329]. A number of patents are taken with regard to the zinc phosphate coatings for its use as corrosion resistant material for metal surfaces [330]. In the color televisions different phosphors are used, for their emission in frequency ranges corresponding to each of the primary colors. The decay time of the phosphor is vital in these applications, with the relevant time scale imposed by the time for the electron beam to sweep the phase of the tube. Zinc phosphate doped with manganese is a well-known phosphor used in cathode tubes [331].

Generally violet colored cobalt pigments are called cobalt violet. First developed in the early 19th century, cobalt violet was the primary permanent violet pigment available. Cobalt violets range from deep to pale shades with

either a pink or blue hue. The first cobalt violets used were composed of cobalt arsenate. This highly toxic compound is now rarely used. Instead most current cobalt violets are non-toxic and are made from either cobalt phosphate, or cobalt ammonium phosphate. Cobalt violets are used in paints [332**].**

Nowadays nanostructured tungstate materials have aroused much interest because of their luminescence behaviour, structural properties and potential applications in the fields of microwave and catalysis. They are also used as optical fibres, scintillator materials and humidity sensors. Studies on the luminescence center excited state absorption in tungstates have been reported [333]. Large arrays of scintillating crystals have been assembled for precision measurements of photons and electrons in high energy and nuclear physics. Single crystals of lead tungstate were chosen by the compact muon solenoid experiment in constructing a precision electromagnetic calorimeter at the Large Hadron Collider because of its high density and fast decay time [334].

$PbWO_4$ with a tetragonal scheelite structure is of technological importance because of its high density, short decay time, high irradiation damage resistance, interesting excitonic luminescence, thermoluminescence and stimulated Raman scattering behavior [335].

Different methods for the synthesis and morphology control of $PbWO_4$ nano and microcrystals have been reported [336-339]. Studies on yttrium doped single crystal $PbWO_4$ [340-342], study of the electronic structures of scheelite and scheelite-like $PbWO_4$ [343], first-principles study on the electronic structures of $PbWO_4$ crystals [344,345], high-pressure X-ray and neutron powder diffraction study of $PbWO_4$ and $BaWO_4$ scheelites [346], and studies on light yield improvement in $PbWO_4$ crystals have also been reported [347].

Several groups have investigated heat capacity studies of silver tungstate, kinetics and mechanisms of solid-state re-actions of silver tungstate with mercuric bromoiodide and mercuric chlorobromide and also the solid-state reactions of silver tungstate with mercuric bromide and mercuric chloride [348-350].

Among the tungstate crystals, $BaWO_4$ crystals are widely used for electro optics due its emission of blue luminescence ascribed to the influence of the Jahn-Teller effect on the degenerated excited state of the $(WO_4)^{2-}$ tetrahedral structure [351]. It is instructive to study the synthesis and physical properties of barium tungstate which is also a potential material for designing solid–state lasers emitting radiation in a specific spectral region and is regarded as a promising wide range Raman active crystal [352, 353]. Numerous efforts have undertaken by different groups over the years for the synthesis of $BaWO_4$ crystals by, polymer micelle –assisted method [354], shape controlled synthesis using different surfactants [355], template free precipitation technique [356], polymeric catanionic reverse micelles method [357], employment of supramolecular templates [358], hydrothermal and electrochemical synthesis [359, 360].

Most of these methods require high temperature heating. At high temperature there is a tendency for the WO_3 group to evaporate, resulting inhomogeneous composition of tungstates. Phosphors prepared by wet chemical method have higher uniformity in particle size distribution with good crystallanity and exhibit higher photoluminescent intensity than those of the solid-state reaction prepared [361, 362]. In chemical precipitation, the kinetics of nucleation and particle growth in homogeneous solutions can be adjusted by the controlled release of the anions and cations. The particle size is influenced by the reactant concentration, pH and temperature [363].

Given the importance of oxide materials, it is only natural to explore "user- friendly" techniques for the synthesis of these materials. Recently there are many developments in the preparation and use of nanoparticulate oxide materials, more specifically isolated nanoparticles of simple and compound oxides. Even though oxide nanoparticles have been known and studied for many decades, it is only in recent years that methods for their preparation have achieved the level of sophistication, which permits monodisperse nanoparticles to be produced in quantity. The emphasis is on new routes for the preparation of oxide nanoparticles, and how these could be distinct from those used for metals or chalcogenides.

Assembling nanoparticles to form nanostructures is a complex process. The synthetic methods have many disadvantages and only a very few can be considered as "user- friendly". Most of the methods require high temperature and solid templates. Majority of the raw materials used are extremely toxic, unstable and expensive. Some methods require sophisticated equipments and inert atmospheres. Also the reactions are not easy to control or to reproduce and have no diversity. Many of them generate a lot of pollutants harmful to the environment. Hence alternative routes should include less expensive and simpler approaches with diversity, which are environmentally benign. It is important to consider the consumption of raw materials and energy and the generation of waste when a synthesis procedure is designed whether it is an original one or an alternative approach. The significance of soft-chemical synthesis is in this contest.

In this investigation we have adopted, soft chemical routes like sol-gel method and chemical precipitation for the synthesis of nanostructures of ferrites, vanadates, tungstates and phosphates with varying dimensionality. We have adopted these synthetic routes since these methods are eco-friendly,

energy saving and highly reproducible. These ternary oxide materials are selected for the present study because of their inherent stability after synthesis and due to their potential applications in the fields of magnetism, catalysis and luminescence**.**

- ✶ The second chapter gives a specific review on ternary oxide materials like ferrites, vanadates, tungstates and phosphates**.**
- ✶ The third chapter describes synthesis of copper ferrite and cobalt ferrite nanoparticles by sol-gel method, characterization, study of the magnetic and the microwave dielectric and magnetic properties.
- ✶ The fourth chapter deals with synthesis of silver vanadate nanorods and bismuth vanadate nanobars by aqueous room temperature precipitation method, characterization and photocatalytic studies.
- ✶ The fifth chapter describes the morphology tuning of tungstate nanomaterials like, Snowflake-like tetragonal $PbWO_4$ nanocrystals and bamboo leaf-like monoclinic $PbWO_4$ nanocrystals, rod-like and fibre-like silver tungstate (Ag_2WO_4) nanocrystals,) Cactus and Aloe Vera leaf-like $BaWO_4$ nanocrystals by room temperature precipitation method, characterization and studies.
- ✶ The sixth chapter focuses on synthesis of zinc orthophosphate and cobalt orthophosphate nanoplatelets by aqueous room temperature precipitation method, characterization and studies.
- ✶ The seventh chapter is the conclusions and future outlook of our research work.

1.9. References

1. A.S. Edelstein (ed), *Nanomaterials: Synthesis, Properties and Applications*, IOP publishing, Bristol, (1999)
2. Z.Y. Zhang, M.G. Lagally, *Science*, 276 (1997) 377
3. K.P. Jayadevan, T.Y. Tseng, *Encyclopedia of Nanoscience and Nanotechnology*, H.S. Nalwa (ed), American Scientific, California, 8 (2004)
4. J.R. Weertman, R.S. Averback, *Nanomaterials: Synthesis, Properties and Applications*, A.S. Edelstein, R.C. Cammarata (eds), IOP publishing, London, (1996) 323
5. Carl C. Koch (ed), *Nanostructured Materials; Processing, Properties and Applications, (2nd edn.)*, William Andrew Inc., USA, (2007)
6. S. Decker, K.J. Klabunde, *J. Am. Chem. Soc*., 118 (1996) 12465
7. R.W. Siegel, *Mater. Sci. Eng. A*, 168 (1993) 189
8. A.P. Alivisatos, *J. Phys. Chem.*, 100 (1996) 13226
9. Y. Arakawa, H. Sakaki, *Appl. Phys. Lett*., 40 (1982) 939
10. H. Gleiter, *Nanostruct. Mater*., 6 (1995) 3
11. W. Chen, *Handbook of Nanostructured Materials and Nanotechnology; Optical Properties*, H.S. Nalwa (ed), Academic Press, New York, 4 (2000)
12. M.D. Sacks, T.Y. Tseng, *J. Am. Ceram. Soc*., 67 (1984) 526
13. J.A. Switzer, C.J. Hung, L.Y. Huang, E.R. Switzer, D.R. Kammler, T.D. Golden, E.W. Bohannan, *J. Am. Chem. Soc*., 120 (1998) 3530
14. J.H. Fendler, *Chem. Mater*., 13 (2001) 3196
15. G.H. Beall, L.R. Pinckney, *J. Am. Ceram. Soc*., 82 (1999) 5

16. M.Y. Lin, H.M. Lindsay, D.A. Weitz, R.C. Ball, R. Klein, P. Meakin, *Proc. Roy. Soc. London, Ser. A.*, 423 (1989) 71
17. B.B. Mandelbrot, *The Fractal Geometry of Nature*, Freeman, Sanfrancisco, (1983)
18. J.K. Kjems, A. Bunde, S. Havlin (eds), *Fractals and Disordered systems*, Springer- Verlag, New York, (1996)
19. L.W. Miller, M.I. Tejedor, B.P. Nelson, M.A. Anderson, *J. Phys. Chem. B*, 103 (1999) 8490
20. P. Yang, D. Zhao, D.I. Margolese, B.F. Chmelka, G.D. Stucky, *Chem. Mater*., 11 (1999) 2813
21. D.N. Srivastava, N. Perkas, A. Gedanken, I. Felner, *J. Phys. Chem. B*, 106 (2002) 1878
22. A.R. West, *Solid State Chemistry and Its Applications*, John Wiley & Sons, New York, (1984)
23. A.Z. Zakhidov, R.H. Boughman, Z. Iqbal, C. Cui, I. Khyyrullin, S.O. Dantas, J. Marti, V.G. Ralchenko, *Science*, 282 (1998) 897
24. J.E.G.J. Wijnhoven, W. Vos, *Science*, 281 (1998) 802
25. B.T. Holland, C.F. Blanford, A. Stein, *Science*, 281 (1998) 538
26. L. Smart, E. Moore, *Solid State Chemistry; an Introduction (2nd edn.)*, Nelson Thornes, U.K., (2004)
27. A. Dyer, *An Introduction to Zeolite Molecular Sieves*, John Wiley, New York, (1988)
28. S. Iijima, *Nature*, 354 (1991) 56
29. X. Feng, G.E. Fryxel, L.Q. Wang, A.Y. Kim, J. Liu, K.M. Kemner, *Science*, 276 (1997) 923
30. U. Bach, D. Lupo, P. Comte, J.E. Moser, F. Weissortel, J. Salbeck, H. Spreitzer, M. Gratzel, *Nature*, 395 (1998) 583

31. W.Q. Han, S.S. Fan, Q.Q. Li, Y.D. Hu, *Science*, 277 (1997) 1287
32. H. Dai, J.H. Hafner, A.G. Rinzler, D.T. Colbert, R.E. Smalley, *Nature*, 384 (1996) 147
33. S. Frank, P. Poncharal, Z.L. Wang, W.A. De Heer, *Science*, 280 (1998) 1744
34. S. Iijima, *Nature*, 354 (1991) 54
35. G.M. Wang, E.M. Sevick, E. Mittag, D.J. Searles, D.J. Evans, *Phys. Rev. Lett*., 89 (2002) 50601
36. P.V. Braun, P. Osenar, S.I. Stupp, *Nature*, 380 (1996) 325
37. W.D. Luedike, U. Landman, *Adv. Mater*., 8 (1996) 428
38. I.S. Yin, Z.L. Wang, *Phys. Rev. Lett*., 79 (1997) 2570
39. S. Sun, C.B. Murray, *J. Appl. Phys*., 85 (1999) 4325
40. Z.L. Wang, *Adv. Mater*., 10 (1998) 13
41. S.A. Harlenist, Z.L. Wang, M.M. Alvarez, I. Vezmar, R.L. Whetten, *J. Phys. Chem*., 100 (1996) 13904
42. J.W. McBain, C.S. Salmon, *J. Am. Chem. Soc*., 43 (1920) 426
43. H. Gutmann, A.S. Kertes, J. *Colloid Interface Sci*., 51 (1973) 406
44. M.P. Pileni, I. Lisiecki, *J. Am. Chem. Soc*., 115 (1993) 3887
45. Z.J. Chen, X.M. Qu, F.Q. Fang, L. Jiang, *Colloids Surf. B*, 7 (1996) 173
46. J.C. Love, L.A. Estroff, J.K. Kriebel, R.G. Nuzzo, G.M. Whitesides, *Chem. Rev*., 105 (2005) 1103
47. D.V. Talapin, R. Koeppe, S. Goetzinger, A. Kornowski, M. Haase, H. Weller, *Nano Lett*., 1 (2001) 207
48. I. Mekis, D.V. Talapin, A. Kornowski, M. Haase, H. Weller, *J. Phys. Chem. B*, 107 (2003) 7454

49. X. Chen, Y. Lou, C. Burda, *Ind. J. Nanotech*., 1 (2004) 105
50. H. Zeng, J. Li, Z.L. Wang, J.P. Liu, S. Sun, *Nano Lett*., 4(1) (2004) 187
51. S. Kim, B. Fisher, H. Eisler, M. Bawandi, *J. Am. Chem. Soc*., 125 (2003) 11466
52. M. Sarikaya, *Proc. Nat. Acad. Sci*., USA, 96 (1999) 14183
53. R.B. Frankel, D.A. Bazilinski, *Hyperfine interact*, 90 (1994) 135
54. R. Narayanan, M.A. El-Sayed, *Nano Lett*., 4(7) (2004) 1343
55. Y. Li, M.A. El-Sayed, *J. Phys. Chem. B*, 105 (2001) 8938
56. D. Fischer, A. Curioni, W. Andreoni, *Langmuir*, 19 (2003) 3567
57. D.J. Lavrich, S.M. Wetterer, S.L. Bernasek, G.J. Scoles, *Phys. Chem. B*, 102 (1998) 3456
58. J. Maier, *Solid State Ionics*, 23 (1987) 59
59. L.E. Brus, *J. Chem. Phys*., 80 (1984) 4403
60. S. Li, S.J. Silvers, M.S. El-Shall, *Mater. Res. Symp. Proc*., 452 (1997) 389
61. H. Gleiter, *Prog. Mater. Sci*., 33 (1989) 223
62. J. Rupp, R. Birringer, *Phys. Rev. B*, 36 (1987) 7888
63. Ph. Buffat, J. P. Borel, *Phys. Rev. A*, 13 (1976) 2287
64. Z.L. Wang (ed), *Characterization of Nanophase Materials*, Wiley-VCH, New York, (2000)
65. J. Karch, R. Birringer, H. Gleiter, *Nature*, 330 (1987) 556
66. L. Gunther, *Phys. World*, 3 (1990) 28
67. R.G. L. Audran, A.P. Huguenard, *U. S. Patent*, 4302523 (1981)
68. R.F. Ziolo, *U.S. Patent*, 4474866 (1984)

69. R.H. Marchessault, S. Ricard, P. Rioux, *Carbohydrate Res*., 224 (1992) 133

70. R.D. Mc Mickael, R.D. Shull, L.J. Swartzendruber, L.H. Bennett, R.E. Watson, *J. Magn. Magn. Mater*., 111 (1992) 29

71. L. Anton, *J. Magn. Magn. Mater*., 85 (1990) 219

72. M.N. Baibich, J.M. Broto, A. Fert, F.N. Van Dau, F. Petroff, P. Etienne, G. Creuzet, A. Friederich, J. Chazelas, *Phys. Rev. Lett*., 61 (1988) 2472

73. S. Jin, T.H. Tiefel, M. Mc Cormack, R.A. Fastnacht, R. Ramesh, L. H. Chen, *Science*, 264 (1994) 413

74. G.J. Thomas, R.W. Siegel, J.A. Eastman, *Scr. Metall. Mater*., 24 (1990) 201

75. K. Sattler, G. Raina, M. Ge, N. Venkateswaran, J. Xhie, Y.X. Liao, R.W. Siegel, *Appl. Phys*., 76 (1994) 546

76. S. Ramasamy, J. Jiang, H. Gleiter, R. Birringer, U. Gonser, *Solid State Commun*.,74 (1990) 851

77. D. Wolf, J.F. Lutsko, *Phys. Rev. Lett*., 60 (1988) 1170

78. B.D. Cullity, *Elements of X-ray Diffraction*, Addison-Wesley, New York, (1978)

79. P. Gao, H. Gleiter, *Acta. Metall*., 35 (1990) 1571

80. W.W. Milligan, S.A. Hackney, M. Ke, E.C. Aifantis, *Nanostruct. Mater*., 2 (1993) 267

81. R.W. Siegel, G.L. Trigg (eds), *Encyclopedia of Applied Physics*, VCH, Weinheim, 11 (1994)

82. R.W. Siegel, G.E. Fougere, *Mater. Res. Symp. Proc*., 362 (1995) 219

83. R.W. Siegel, *Nanomaterials: Synthesis, Properties and Applications*, A.S. Edelstein, R.C. Cammarata (eds), IOP publishing, Philadelphia, (1998)
84. M. Figlarz, *Chem. Scripta*., 28 (1988) 28
85. J. Rouxel (ed), *Soft Chemistry Routes to New Materials,* Materials Science Forum, Trans Tech Switzerland, 152-153 (1994)
86. D.C. Bradely, R.C. Mehrotra, D.P. Gaur, *Metal Alkoxides*, Academic Press, London, (1990)
87. I.A. Aksay, *Forming of Ceramics, Advances in Ceramics*, J.A. Mangals, G. L. Messing (eds), Am. Ceram. Soc., Columbus, Ohio, 9 (1984)
88. Y.X. Huang, C. Guo, *J. Powder Technol*., 72 (1992) 101
89. H. Yamamura, *Ceram. Int*., 11 (1985) 72
90. H.S. Potdar, S.B. Deshpande, S.K. Date, *Mater. Chem. Phys*., 58 (1999) 121
91. L. Spanhel, M. Haase, H. Weller, A. Henglein, *J. Am. Chem. Soc*., 109(19) (1987) 5649
92. M.T. Harrison, S.V. Kershaw, M.G. Burt, A. Rogach, A. Eychmuller, H.J. Weller, *Mater. Chem*., 9(11) (1999) 2721
93. M. Gao, B. Richter, S. Kirstein, H. Moehwald, *J. Phys. Chem. B*, 102(21) (1998) 8360
94. S. Somiya, R. Roy, *Bull. Mater. Sci*., 23 (2000) 453
95. W.J. Dawson, *Am. Ceram. Soc. Bull*., 67 (1988) 1673
96. A.M. Milia, *Sonochemistry and Cavitation*, Gordon and Breach Publishers, Luxemborg, (1995)
97. S. Komerneni, R. Pidugu, Q.H. Li, R. Roy, *J. Mater. Res*., 10 (1995) 1687

98. F.B. Landry, D.V. Basile, G. Spenlehauer, M. Veillard, J. Kreuter, *Biomaterials*, 17 (1996) 715

99. Z. Kiraly, I. Dekany, A. Mastalir, M. Bartok, *J. Catalysis*, 161 (1996) 401

100. V. Degiorgio, M. Corti (eds), *Physics of Amphiphilic Micelles, Vesicles and Microemulsions*, North Holland, Amsterdam, (1985)

101. J.A.L. Perez, M.A.L. Quintela, J. Mira, J. Rivas, S.W. Charles, *J. Phys. Chem. B*, 101 (1997) 8045

102. J. Wang, J. Fang, L.M. Gan, S.C. Ng, J. Ding, X. Liu, *J. Am. Ceram. Soc*., 83 (2000) 1049

103. B.K. Paul, S.P. Moulik, *J. Dispersion Sci. Tech*., 18 (1997) 301

104. A. Chevreau, B. Philips, B.G. Higgins, S.H. Risbuds, *J. Mater. Chem*., 6 (1996) 1643

105. E. Kumacheva, O. Kalinina, L. Lilge, *Adv. Mater*., 11 (1999) 231

106. J.C. Neal, S. Stolnik, E. Schacht, E.R. Kenawy, M.C. Garnett, S.S. Davis, L. Illum, *Pharm. Sci*., 87 (1998) 1242

107. N. Suzuki, S. Kimura, Y. Saito, C. Kaito, *Phys. Low Dimen. Struct*., 3-4 (1998) 55

108. W.P. Cai, H.C. Zhong, L.D. Zhang, *J. Appl. Phys*., 83 (1998) 1705

109. D. Vollath, K.E. Sickafus, R. Varma, *Mater. Res. Soc. Symp. Proc*., 269 (1992) 379

110. D. Vollath, *J. Mater. Sci*., 25 (1990) 2227

111. M.T. Harris, T.C. Scott, C.H. Byres, *Mater. Sci. Eng. A*, 168 (1993) 125

112. W. Cai, L. Zhang, *J. Phys. Condensed Matter*, 9 (1997) 7257

113. L. Maya, M. Paranthaman, T. Thundat, M.L. Bauer, J. Vac. *Sci. Technol. B*, 14 (1996) 15

114. W. Li, L. Gao, J.K. Guo, *Nanostruct. Mater*., 10 (1998) 1043

115. D. Indackers, C. Janzen, B. Rellinghaus, *Nanostruct. Mater*., 10 (1998) 247

116. J.M. Nedeljkovic, Z.V. Saponjic, Z. Rakocevic, V. Jokanovic, D.P. Uskokovic, *Nanostruct. Mater*., 9 (1997) 125

117. A.S. Gandhi, V. Jayaram, A.H. Chokshi, *J. Am. Ceram. Soc*., 82 (1999) 2613

118. F. Li, H.G. Zheng, D.Z. Jia, X.Q. Xin, Z.L. Xue, *Mater. Lett*., 53 (2002) 283

119. F. Li, L.Y. Chen, Z.Q. Chen, J.Q. Xu, J.M. Zhu, X.Q. Xin, *Mater. Chem. Phys*., 73 (2002) 335

120. K. Kimoto, Y. Kamiya, M. Nonoyama, R. Uyeda, *Jpn. J. Appl. Phys*., 2 (1963) 702

121. N. Wada, *Jpn. J. Appl. Phys*., 6 (1967) 553

122. N. Wada, *Jpn. J. Appl. Phys*., 7 (1968) 1287

123. I. Nishida, *J. Phys. Soc. Jpn*., 26 (1969) 1225

124. Y. Saito, *Surf. Rev. Lett*., 3 (1996) 819

125. A. Yasuda, N. Kawase, F. Banhart, W. Mizutani, T. Shimizu, H. Tokumoto, *Phys. Chem. B*, 106 (2002) 1247

126. H. Abe, S. Yamamoto, A. Miyashita, K.E. Sickafus, *J. Appl. Phys*., 90 (2001) 3353

127. D. Besset, P. Matteazzi, F. Miani, *Mater. Sci. Eng. A*, 168 (1993) 149

128. K. Shantha, G.N. Subbanna, K.B.R. Varma, *J. Solid State Chem*., 142 (1999) 41

129. M. Emas, H. Nyqvist, *Ind J. Pharm*., 197 (2000) 117

130. E.E. Hassan, A.G. Eshra, A.H. Nada, *Ind J. Pharm*., 121 (1995) 149

131. P. Ravindranathan, K.C. Patil, *Am. Ceram. Soc. Bull*., 66 (1987) 688

132. T. Mimani, K.C. Patil, *Mater. Phys. Mech*., 4 (2001) 134

133. S. Li, S.J. Silvers, M.S. El Shall, *Mater. Res. Symp. Proc*., 452 (1997) 389

134. T.T. Kodas, M.J.H. Smith, *Aerosol Processing of Materials*, Wiley-VCH, New York, (1999)

135. S.K. Friedlander, *Smoke, Dust and Haze: Fundamentals of Aerosol Behaviour*, Wiley Interscience, New York, (1977)

136. R.W. Siegel, *Physics of New Materials,* F.E. Fujitha (ed), Springer-Verlag, Berlin, (1994)

137. A. Gurav, T. Kodas, T. Pluym, Y. Xiong, *Aerosol Sci. Technol*., 19 (1993) 411

138. M.K. Wu, R.S. Windeler, C.K.R. Steiner, T. Bors, S.K. Friedlander, *Aerosol Sci. Technol*., 19 (1993) 527

139. S.E. Pratsinis, T.T. Kodas, *Aerosol Measurement*, K. Willeke, P.A. Baron (eds), Van Nostrand Reinhold, New York, (1993)

140. K.S. Suslick, G.J. Price, *Annu. Rev. Mater. Sci*., 29 (1999) 295

141. K.S. Suslick, S.B. Choe, A.A. Cichowlas, M.W. Grinstaff, *Nature*, 353 (1991) 414

142. Y. Li, X.M. Hong, D.M. Collard, M.A. El Sayed, *Org. Lett*., 2(15) (2000) 2385

143. X. Fu, Y. Wang, N. Wu, L. Gui, Y. Tan, *Langmuir*, 18 (2002) 4619

144. A. Hengelin, *J. Phys. Chem. B,* 104 (2000) 2201

145. R. Narayanan, M.A. El-Sayed, *J. Phys. Chem. B*, 108 (2004) 8572

146. M. Tamura, H. Fugihara, *J. Am. Chem. Soc*., 125(51) (2003) 15742

147. S.H. Wu, D.H. Chen, *Chem. Lett*., 33(4) (2004) 406

148. X. Zhang, K.Y. Chang, *Chem. Mater*., 15(2) (2003) 451
149. A. Harriman, J.M. Thomas, G.R. Millward, *New J. Chem*., 11 (1987) 757
150. S. U. Son, I.K. Park, J. Park, T. Hyeon, *Chem. Commun*., 7 (2004) 778
151. M. Michaelis, A. Henglein, *J. Phys. Chem*., 96 (1992) 4719
152. T. Fujimoto, Y. Mizukoshi, Y. Nagata, Y. Maeda, R. Oshima, *Scr. Mater*., 44 (2001) 2183
153. D. De Caro, J.S. Bradley, *New J. Chem*., 22 (1998) 1267
154. G.T. Cardenas, R.C. Oliva, *Mater. Res. Bull*., 35 (2000) 2227
155. M.T. Reetz, W. Helbig, *J. Am. Chem. Soc*., 116 (1994) 7401
156. R. Narayanan, M.A. El-Sayed, *J. Am. Chem. Soc.*, 126(23) (2004) 7419
157. Z. Lu, G. Liu, H. Philips, J.M. Hill, J. Chang, R.A. Kydd, *Nano Lett*., 1(12) (2001) 683
158. K. Esumi, R. Isono, T. Yoshimura, *Langmuir*, 20(1) (2004) 237
159. S. Chen, K. Kimura, *J. Phys. Chem. B*, 105 (2001) 5397
160. B.F.G. Johnson, *Top. Catal*., 24 (2003) 147
161. M. Harutha, *Chem. Rec*., 3(2) (2003) 75
162. Z. Liu, X.Y. Ling, X. Su, J.Y. Lee, *J. Phys. Chem. B*, 108 (2004) 8234
163. A.G. Boudjahem, S. Monteverdi, M. Mercy, M.M. Bettahar, *J. Catal*., 221(2) (2004) 325
164. O. Mamezaki, H, Adachi, S. Tomita, M. Fujii, S. Hayashi, *Jpn. J. Appl. Phys*., 39 (2000) 6680
165. D. Babonneau, T. Cabioc'h, A. Naudon, J.C. Girard, M.F. Denanot, *Surf. Sci*., 409 (1998) 358

166. R. Dietrich, *Pharm. Ind*., 54 (1992) 459

167. T.G. Park, M.J. Alonso, R. Langer, *J. Appl. Polym. Sci*., 52 (1994) 1797

168. P. Luo, T.G. Nieh, *Biomaterials*, 17 (1996) 1959

169. H.M. Pathan, C.D. Lokhande, *Bull. Mater. Sci*., 27 (2004) 85

170. T. Fukui, S. Ando, Y. Tokura, T. Toriyama, *Appl. Phys. Lett*., 58 (1991) 2018

171. T. Tachibana, T. Someya, Y. Arakawa, *Appl. Phys. Lett*., 74 (1999) 383

172. S. Ishida, Y. Arakawa, K. Wada, *Appl. Phys. Lett*., 72 (1999) 800

173. D.P. Yu, X.S. Sun, C.S. Lee, I. Bello, Y.H. Tang, G.W. Zhou, Z.G. Bai, Z. Zhang, S.Q. Feng, *Solid State Commun*., 105 (1998) 403

174. H.Z. Zhang, D.P. Yu, Y. Ding, Z.G. Bai, H.L. Hang, S.Q. Feng, *Appl. Phys. Lett*., 73 (1999) 3396

175. P.X. Gao, Y. Ding, Z.L. Wang, *Nano Lett*., 3 (2003) 1315

176. Z.R. Dai, Z.W. Pan, Z.L. Wang, *J. Phys. Chem. B*, 106(5) (2002) 902

177. Z.R. Dai, J.L. Gole, J.D. Stout, Z.L. Wang, *J. Phys. Chem. B*, 106(6) (2002) 1274

178. N.C. Manekar, P.K. Puranik, S.B. Joshi, *J. Microencapsulation*, 8 (1991) 521

179. N.B. Dharamadhikari, S.B. Joshi, N.C. Manekar, *J. Microencapsulation*, 8 (1991) 479

180. P.B. Deasy, *Crit. Rev. Therapeutic Drug Carrier Syst*., 8 (1991) 39

181. B.D. Cullity, S.R. Stock, *Elements of X-ray Diffraction* (*3rd edn.*), Prentice Hall, Upper Saddle River, NJ, (2001)

182. C. Surya Narayana, M. Grant Norton, *X-ray Diffraction a Practical Approach*, Plenum Press, New York, (1998)

183. A.R. West, *Solid State Chemistry and Its Applications*, John Wiley & Sons, Singapore, (2003)

184. R.A. Young (ed), *The Rietveld Method*, Oxford University Press, Oxford, (1996)

185. G. Schmid (ed), *Nanoparticles. From Theory to Applications*, Wiley-VCH, (2004) 208

186. J.W. Edington, *Practical Electron Microscopy in Materials*, Van Nostrand Reinhold, New York, (1976)

187. Z.L. Wang, *Reflected Electron Microscopy and Spectroscopy for Surface Analysis*, Cambridge University Press, Cambridge, (1996)

188. G. Cao, *Nanostructures & Nanomaterials. Synthesis, Properties and Applications*, Imperial College Press, (2004)

189. M. Kohler, W. Fritzsche (eds), *Nanotechnology*, *An Introduction to Nanostructuring Techniques*, Wiley VCH, (2004)

190. A.S. Nowick (ed), *Electron Microscopy of Materials; An Introduction*, Academic Press, New York, (1980)

191. D. Bonnell (ed), *Scanning Probe Microscopy and Spectroscopy*, Wiley-VCH, New York, (2001)

192. D. Sarid, *Scanning Force Microscopy with Applications to Electric, Magnetic and Atomic Forces,* Oxford University Press, New York, (1991)

193. D. Sarid, V. Elings, *J. Vac. Sci. Technol. B*, 9(2) (1991) 431

194. G. Binning, C.F. Quanta, C. Gerber, *Phys. Rev. Lett*., 56 (1986) 930

195. G. Binning, H. Rohrer, C. Gerber, E. Weibel, *Phys. Rev. Lett*., 49 (1982) 57

196. H.P. Long, M. Hegner, E. Meyer, C. Gerber, *Nanotechnology*, 13 (2002) R29

197. J.M. Niemantsverdriet, *Spectroscopy in Catalysis*, VCH Publishers, New York, (1995)

198. S. Foner, *IEEE Trans. Magn*., 17 (1981) 3358

199. S. Foner, *J. Appl. Phys*., 79 (1996) 4740

200. A. Niazi, P. Poddar, A.K. Rastogi, *Current Science*, 79(1) (2000) 99

201. K. Nakamoto, *Infrared and Raman Spectra of Inorganic and Coordination Compounds Part A: Theory and Applications in Inorganic Chemistry (5th edn.),* Wiley- Interscience, New York, (1997)

202. C.N. Banwell, E.M. McCash, *Fundamentals of Molecular Spectroscopy (4th edn.),* McGraw- Hill International, UK, (1999)

203. R.P. Bauman, *Absorption Spectroscopy*, John Wiley, New York, (1965)

204. J.E. Crooks, *The Spectrum in Chemistry*, Academic, New York, (1978)

205. A.R. West, *Basic Solid State Chemistry (2nd edn.),* John Wiley & Sons, Chichester, (2000) (reprinted)

206. D.R. Vij (ed), *Luminescence of Solids*, Plenum Press, New York, (1998)

207. H.S. Nalwa (ed), *Encyclopedia of Nanoscience and Nanotechnology*, American Scientific, California, 4 (2004) 692

208. K.K. Kamath, P.R. Vaya (eds), *Semiconductor Materials Characterization Techniques*, Narosa Publishing House, New Delhi, (1993) 265

209. Y. Wang, N. Herron, *J. Phys. Chem*., 95 (1991) 525

210. K.K. Smith, *Thin Solid films*, 84 (1981) 171

211. D.M. Eagles, *J. Phys. Chem. Solids*, 16 (1960) 76

212. W. Chen, A.G. Joly, S. Wang, *Encyclopedia of Nanoscience and Nanotechnology*, H. S. Nalwa (ed), American Scientific Publishers, California, 4 (2004) 689

213. W. Chen, A.G. Joly, C.M. Kowalchuk, J.O. Malm, Y. Huang, J.O. Bovin, *J. Phys. Chem. B*, 106 (2002) 7034

214. A. Fujishima, T.N. Rao, D.A. Tryk, *J. Photochem. Photobiol.* C, 1(2000) 1

215. V. Augugliaro, M. Litter, L. Palmisano, J. Soria, *J. Photochem. Photobiol. C, Photochem. Rev.*, 7 (2006) 127

216. E. Yassıtepe, H.C. Yatmaz, C. Ozturk, K. Ozturk, C. Duran, *J. Photochem. Photobiol. A: Chemistry*, 198 (2008) 1

217. K.V. Baiju, S. Shukla, K.S. Sndhya, J. James, K.G.K. Warrier, *J. Phys. Chem. C*, 111(2007) 7612

218. Z. Zhang, C.C. Wang, R. Zakaria, J.Y. Ying, *J. Phys. Chem. B*, 102 (1998) 10871

219. R. Wang, J.H. Xin, Y. Yang, H. Liu, L. Xu, *Appl. Surf. Sci*., 227 (2004) 312

220. M. Long, W. Cai, H. Kisch, *J. Phys. Chem. C*, 112 (2008) 548

221. L. Zhou, W.Z. Wang, S.W. Liu, L.S. Zhang, H.L. Xu, W. Zhu, *J. Mol. Catal. A*, 252 (2006) 120

222. L. Zhang, D.R. Chen, X.L. Jiao, *J. Phys. Chem. B*, 110 (2006) 2668

223. S. Kohtani, S. Makino, A. Kudo, K. Tokumura, Y. Ishigaki, T. Matsunaga, O. Nikaido, K. Hayakawa, R. Nakagaki, *Chem. Lett*., 31 (2002) 660

224. R. Ullah, J. Dutta, *J. Hazardous Materials*, 156 (2008) 194

225. A. Fujishima, K. Honda, *Nature*, 238 (1972) 37

226. A. Mills, S.L. Hunte, *Photochem. Photobiol. A*, 108 (1997) 1

227. K. Domen, J.N. Kondo, M. Hara, T. Takata, *Bull. Chem. Soc. Jpn*., 73 (2000) 1307

228. A. Kudo, K. Omori, H. Kato, *J. Am. Chem. Soc*., 121 (1999) 11459

229. S. Tokunaga, H. Kato, A. Kudo, *Chem. Mater*., 13 (2001) 4624

230. A. Kudo, K. Ueda, H. Kato, I. Mikami, *Catal. Lett*., 53 (1998) 229

231. M. Long, W.M. Cai, J. Cai, B.X. Zhou, X.Y. Chai, Y.H. Wu, *J. Phys. Chem. B*, 110 (2006) 20211

232. L. Zhang, D.R. Chen, X.L. Jiao, *J. Phys. Chem. B*, 110 (2006) 2668

233. J.Q. Yu, A. Kudo, *Adv. Funct. Mater*., 16 (2006) 2163

234. J.W. Dodd, K.H. Tonge, *Thermal methods in Analytical Chemistry by Open Learning*, John Wiley & Sons, New York, (1987)

235. T. Hatakeyama, Z. Liu (eds), *Handbook of Thermal Analysis*, John Wiley & Sons, Chichester, (1998)

236. R.C. Mackenzie, *Thermochim. Acta*., 28 (1979) 1

237. R.C. Mackenzie , *Isr. J. Chem*., 22 (1982) 2003

238. W. Wendlant, *Thermal Analysis (3rd edn.)*, John Wiley & Sons, New York, (1986)

239. B. Kumar, G. Srivastava, *J. Appl. Phys.*, 75 (1994) 6115

240. K.T. Mathew, U. Raveendranath, *Sensors Update*, Wiley VCH, Germany, 7 (1999) 185

241. K.T. Mathew, *Perturbation Theory; Encyclopedia of RF and Microwave Engineering*, Wiley-Interscience, USA, 4 (2005) 3725

242. K.T. Mathew, S.B. Kumar, A. Lonappan, J. Jacob, J. Samuel, T. Xavier, T. Kurian, *Mater. Lett.*, 56 (2002) 248

243. K.T. Mathew, S.B. Kumar, A. Lonappan, J. Jacob, T. Kurian, J. Samuel, T. Xavier, *Mater. Chem. Phys.*, 79 (2003) 187

244. R.A. Waldron, *Perturbation Theory of Resonant Cavities*, *Proc. IEE*, 107C, (1960) 272

245. T. George, S. Joseph, S. Mathew, *J. Metastable and Nanocrystalline Materials*, 23 (2005) 141

246. U. Raveendranath, K.T. Mathew, *Microwave and Opt. Lett*., 18 (1998) 241

247. R.F. Harrington, *Time Harmonic Electromagnetic fields*, McGraw-Hill, New York, (1961)

248. D.K. Chakrabarty, *Adsorption and Catalysis by Solids*, Wiley Eastern Ltd, New Delhi, (1991)

249. J. Cheon, J.H. Lee, *Acc. Chem. Res.* 41 (2008) 1630

250. J. Gao, B. Xu, *Nanotoday*, 4 (2009) 37

251. A.K. Gupta, M. Gupta, *Biomaterials*, 26 (2005) 3995

252. J. Gao, H. Gu, B. Xu, *Acc. Chem. Res.* 41(16) (2008) 1565

253. L. Zhou, W.Z. Wang, S.W. Liu, L.S. Zhang, H.L. Xu, W. Zhu, *J. Mol. Catal. A*, 252 (2006) 120

254. J.H. Gao, G.L. Liang, J.S. Cheung, Y. Pan, Y. Kuang, F. Zhao, B. Zhang, X.X. Zhang, E.X. Wu, B. Xu, *J. Am. Chem. Soc*., 13 (2008) 11828

255. H. W. Gu, K.M. Xu, Z.M. Yang, C.K. Chang, B. Xu, *Chem. Commun.*, (2005) 4270

256. P.K. Jain, X. Huang, I.H. El-Sayed, M.A. El-Sayed, *Acc. Chem. Res*., 41 (12) (2008) 1578

257. X. Huang, P.K. Jain, I.H. El-Sayed, M.A. El- Sayed, *Nanomedicine*, 2 (2007) 681

258. X. Huang, I.H. El-Sayed, M.A. El- Sayed, *Cancer Lett.*, 239 (2006) 129

259. U. Kreibig, M. Vollmer, *Optical Properties of Metal Clusters*, Springer, Berlin,25 (1995)

260. S. Link, M.A. El-Sayed, *Annu. Rev. Phys. Chem.* 54 (2003) 331

261. X. Huang, I.H. El-Sayed, W.Qian, M.A. El- Sayed, *J. Am. Chem.. Soc*. 128 (2006) 2115

262. A.M. Gobin, M.H. Lee, N.J. Halas, W.D. James, R.A. Drezek, J.L. West, *Nano Lett*. 7 (2007) 1929

263. X. Michalet, F.F. Pinaud, L.A. Bentolila, J.M. Tsay, S. Doose, J.J. Li, G. Sundaresan, A.M. Wu, S.S. Gambhir, S. Weiss, *Science,* 307 (2005) 538

264. H.W. Gu, R.K. Zheng, X.X. Zhang, B. Xu, *J. Am. Chem. Soc.,* 126 (2004) 5664

265. J.H. Gao, W. Zhang, P.B. Huang, B. Zhang, X.X. Zhang, B. Xu, *J. Am. Chem. Soc*. 130 (2008) 3710

266. I. Willner, E-Katz (eds), *Angrew. Chem. Int*. 39 (2000) 1180

267. M-R. Choi, K.J. Stanton-Maxey, J.K. Stanley, C.S. Levin, R. Bardhan, D. Akin, S. Badve, J. Sturgis, J.P. Robinson, R. Bashir, N.J. Halas, S.E. Clare, *Nano Lett*. 7 (2007) 3759

268. A. Galembeck, O.L. Alves, *Thin Solid Films*, 365 (2000) 90

269. A.J. Haes, R.P.A. Van Duyne, *J. Am. Chem. Soc.,* 124 (2002) 10596

270. M. Zhang, J. Li, *Mater. Today*, 12(6) (2009) 12

271. T. Zhang, S. Mubeen, D. Yoo, N.V. Myung, M.A. Deshusses, *Nanotechnology,* 20 (2009) 255501

272. K. Sayama, A. Nomura, Z. Zou, R. Abe, Y. Abe, H. Arakawa, *Chem. Commun*., (2003) 2908

273. P. Mike, *Mater. Today*, 12(6) (2009) 6

274. K. Sayama, A. Nomura, T. Arai, T. Sugita, R. Abe, M. Yanagida, T. Oi, Y. Iwasaki, Y. Abe, H. Sugihara, *J. Phys. Chem. B*, 110 (2006) 11352

275. H.W. Gu, K.W. Xu, C.J. Xu, B. Xu, *Chem. Commun.,* (2006) 941

276. I. Safarik, M. Safarikova, *Biomagn. Res. Technol.*, 2 (2004) 7

277. C.J. Leroux, *Nat. Nanotechnol.*, 2 (2007) 679

278. H.W. Gu, P.L. Ho, K.W.T. Tsang, L. Wang, B. Xu, *J. Am. Chem. Soc.*, 125 (2003) 15702

279. M.H. Shinkai, H. Honda, T. Kobayashi, *Biocatalysis*, 5 (1991) 61

280. F. Du, J. Liu, Z. Guo, *Mat. Res. Bull.*, 44 (2009) 25

281. S.G. Kwon, T. Hyeon, *Acc. Chem. Res.*, 41(12) (2008)1696

282. G. Schmid (ed), *Clusters and Colloids. From Theory to Applications*, VCH, Weinheim, (1994)

283. K.L. Lee, E.E. Wolf, *Catal. Lett*. 26 (1994) 297

284. L.M. Liz-Marzan, P.V. Kamat (eds), *Nanoscale Materials*, Kluwer Academic Publishers, Boston, (2003)

285. J.L. Plawsky, R. Achanta, W. Cho, D. Rodriguez, R. Saxena, W.N. Gill, *Dielectric Films for Advanced Microelectronics*, M. Baklanov, M. Green, K. Maex (eds), Wiley & Sons, London, (2007)

286. A. Jain, S. Rogojevic, S. Ponoth, N. Agarwal, I. Matthew, W.N. Gill, P. Persans, M. Tomozawa, J.L. Plawsky, E. Simonyi, *Thin Solid Films*, 398-399 (2001) 513

287. D. Konjhodzic, S. Schroter, F. Marlow, *Phys. Status Solidi (a)*, 204 (2007) 3676

288. D.J. Poxson, M.F. Schubert, F.W. Mont, E.F. Schubert, J.K. Kim, *Opt. Lett.*, 34 (2009) 728

289. J.K. Kim,S.Chhajed, M.F. Schubert, E.F. Schubert, A.J. Fischer, M.H. Crawford, J. Cho, H. Kim, C. Sone, *Adv. Mater.*, 20(4) (2008) 801

290. A. Sleight, *Science*, 242 (1988) 1519

291. Lubkin, B. Gloria, *Physics Today*, 49 (1996) 48

292. H.W. Kroto, J.R. Heath, S.C. O'Brien, R.F. Curl, R.F. Smalley, *Nature*, 318 (1985) 162

293. A. Govindaraj, C.N.R. Rao, *The Chemistry of Nanomaterials, (Nanotubes and Nanowires)*, C.N.R. Rao, A. Muller, A.K. Cheetham (eds), Wiley-VCH, Weinheim, 1 (2004)

294. K. Kageyama, J. Tamazawa, T. Aida, *Science*, 285 (1999) 2113

295. S. Jin, T.H. Tiefel, M. McCormack, R.A. Fastnacht, R. Ramech, L.H. Chen, *Science*, 264 (1994) 413

296. H. Goronkin, P. Von Allmen, R.K. Tsui, T.X. Zhu, *WTEC Panel Report on Nanostructure Science and Technology*, R. W. Siegel, E. Hu, M.C. Roco (eds), Kluwer Academic Publishers, Dordrecht, Netherlands, (1999)

297. A.I. Kingon, J.P. Maria, S.K. Streiffer, *Nature*, 406 (2000) 1032

298. R.J. Cava, *J. Am. Ceram. Soc.*, 83 (2000) 5

299. J.Z. Sun, A. Gupta, *Annu. Rev. Mater. Sci*., 28 (1998) 45

300. J.F. Scott, *Annu. Rev. Mater. Sci*., 28 (1998) 79

301. O. Auciello, J.F. Scott, R. Ramesh, *Physics Today*, July (1998) 22

302. D. Dimos, C.H. Mueller, *Annu. Rev. Mater. Sci*., 28 (1998) 397

303. B.C.H. Steele, A.K. Heinzel, *Nature*, 414 (2001) 345

304. J.M. Tarascon, M. Armand, *Nature*, 414 (2001) 359

305. R. Seshadri, *The Chemistry of Nanomaterials, (Oxide Nanoparticles)*, C.N.R. Rao, A. Muller, A.K. Cheetham (eds), Wiley-VCH, Weinheim, 1 (2004)

306. C.N.R. Rao, B. Raveau, *Transition Metal Oxides*, VCH Publishers Inc., New York, (1995)

307. J.L.G. Fierro, *Metal Oxides: Chemistry and Applications*, CRC Press, Boca Raton, FL, (2006)

308. M. Niederberger, *Acc. Chem. Res.*, 40 (2007) 793

309. X-H Huang, Z-H Chen, *Solid State Commun*., (2004) 132

310. C.G. Ramankutty, S. Sugunan, *Applied Catalysis A: General*, 218 (2001) 39

311. S. Bhattacharyya, J-P Salvetat, R. Fleurier, A. Husmann, T. Cacciaguerra, M-L. Saboungi, *Chem. Commun.*, (2005) 4818

312. M.A. Ahmed, M.K. Elnimer, A. Tawtic and A.M. El. Hasab, *J. Magn. Magn. Mater.* 98 (1991) 33

313. S. Krupanicha, *The Physics of Ferrites and Magnetic Oxides Related to Them (Russian translation) (1st edn.)*, Mir, Moscow, (1976)

314. G. Ji, S. Tang, B. Xu, B. Gu, Y. Du, *Chem. Phys. Lett.*, 379 (2003) 484

315. D.E. Zhang, X.J. Zhang, X.M. Ni, J.M. Song, H.G. Zheng, *J. Magn. Magn. Mater*., 305 (2006) 68

316. K.J. Takeuchi, A.C. Marschilok, S.M. Davis, R.V. Leising, E.S. Takeuchi, *Coord. Chem. Rev.*, 219-221 (2001) 283

317. W.I.F. David, I.G. Wood, *J. Phys. C: Solid State Phys.*, 16 (1983) 5149

318. A.R. Lim, S.H. Choh, M.S. Jang, *J. Phys: Condens. Matter,* 7 (1995) 7309

319. J.D. Bierlein, A.W. Sleight, *Solid State Commun.*, 16 (1975) 69

320. A.R. Lim, J.H. Chang, S.H. Choh, *Phys. Status Solidi B*, 196 (1996) 33

321. P.P. Man, S.H. Choh, Fraissard, *J. Solid State Nucl. Magn. Reson.*,3 (1994) 23

322. H.T. Jeong, S.Y. Jeong, W.T. Kim, D.H. Kim, *J. Phys. Soc. Jpn.*, 69(2) (2000) 306

323. S. Tokunaga, H. Kato, A. Kudo, *Chem. Mater*., 13 (2001) 4624

324. M.A. Lopez-Quintela, *J. Colloid Interface Sci.*, 158 (1993) 446

325. H. Nariai, S. Shibamoto, H. Maki, I. Motooka, *Phosphorus Res. Bull.*, 8 (1998) 101.

326. H. Onoda, H. Nariai, H. Maki, I. Motooka, *Phosphorus Res. Bull.,* 9 (1999) 69

327. M. Dinamani, P. Vishnukamath, *Mater. Res. Bull.*, 36 (2001) 2043

328. J.E. Marion, M.J. Weber, Eur. *J. Solid State Inorg.* Chem., 28 (1991) 271

329. H. Engqvist, J.E.S. Walz, J. Loof, G.A. Botton, D. Mayer, M.W. Phaneul, N.O.Ahnfelt, L. Hermansson, *Biomaterials,* 25 (2004) 2781

330. H.S. Bender, G.D. Cheever, J.J. Wojtkowiak, *Progress in Organic Coatings,* Elsevier Sequoia S.A., Lausanne, Switzerland, 8 (1980) 241

331. W.D. Kingery, H.K. Bowen, D.R. Uhlmann, *Introduction to Ceramics (2nd edn.),* John Wiley and Sons, New York, (1976) 689

332. C.A. Hogarth, M.J. Basha, *J. Phys. D: Appl. Phys.,* 16 (1983) 869-878

333. V. Pankratov, L. Grigorjeva, D. Millers, S. Chernov, A.S. Voloshinovskii, *J. Lumin.,* 94-95 (2001) 427

334. A. Annenkov, E. Auffray, M. Korzhik, P. Lecoq, J.P. Peigneux, *Phys. Status Solidi* 170 (1998) 47

335. X.L Hu, Y.J. Zhu, *Langmuir,* 20 (2004) 1521

336. J. Geng, Y. Lv, D. Lu, J-J Zhu, *Nanotechnology,* 17 (2006) 2614

337. X. He, M. Cao, *Nanotechnology*, 17 (2006) 3139

338. A. Dias, V.S.T. Ciminelli, *Chem. Mater.*, 15 (2003) 1344

339. G. Zhou, M. Lu, F. Gu, D. Xu, D. Yuan, *J. Cryst. Growth,* 276 (2005) 577

340. D. Chen, G. Shen, K. Tang, Z. Liang, H. Zheng, *J. Phys. Chem. B*, 108 (2004) 11280

341. R. Mao, J. Chen, D. Shen, Z. Yin, *J. Cryst. Growth,* 265 (2004) 518

342. J. Xie, P. Yang, H. Yuan, J. Liao, B. Shen, Z. Yin, D. Cao, M. Gu, *J. Cryst. Growth*, 275 (2005) 474

343. Y. Huang, H.J. Seo, Q. Feng, S. Yuan, *Mater. Sci. Eng. B*, 121 (2005) 103

344. Y. Zhijun, L. Tingyu, Z. Qiren, S. Yuanyuan, *Phys. Status Solidi (b)*, 243 (2006) 1802

345. L. Tingyu, S. Jianqi, Z. Qiren, *Solid State Commun.*, 135 (2005) 382-385

346. Z. Yi, T. Liu, Q. Zhang, Y. Sun, *J. Electronic Spect. Related Phenomena*, 151 (2006) 140-143

347. A. Grzechnik, W.A. Crichton, W.G. Marshall, K. Friese, *J. Phys. Condens. Matter*. 18 (2006) 3017-3029

348. N.V. Klassen, N.P. Kobelev, G.K. Strukova, *Nucl. Instrum. Methods Phys. Res. A*, 537 (2005) 177-181

349. P.H. Bottlebergs, H. Everts, G.H.J. Broers, *Mater. Res. Bull.*, 11 (1976) 263

350. P.G. Hall, D.A. Armitage, R.G Linford, *J. Chem. Thermodyn.*, 17 (1985) 657

351. M.A. Beg, A. Jain, *Polyhedron*, 11 (1992) 2775

352. A. Jain, M.A. Beg, *Polyhedron*, 14 (1995) 2293

353. Y. Mao, S.S. Wong, *J. Am. Chem. Soc.*, 126 (2004) 15245

354. Y.F. Chen, K.W. Su, *Opt. Lett.*, 30 (2005) 35

355. P. Cerny, H. Jelinkova, *Opt. Lett.*, 27 (2002) 360

356. G. Zhou, M. Lu, Z. Xiu, S. Wang, H. Zhang, W. Zou, *J. Cryst. Growth*, 276 (2005) 116

357. B. Xie, Y. Wu, Y. Jiang, F. Li, J. Wu, S. Yuan, W. Yu, Y. Qian, *J. Cryst. Growth*, 235 (2002) 283

358. X. Wang, H. Xu, H. Wang, H. Yan, *J. Cryst. Growth*, 284 (2005)

359. H. Shi, X, Wang, N. Zhao, J. Ma, *J. Phys. Chem. B*, 110 (2006) 748

360. J. Liu, Q. Wu, Y. Ding, *Crystal Growth & Design,* 5 (2005) 445

361. W. S. Cho, M. Yoshimura, *Jpn. J. Appl. Phys.*, 36 (1997) 1216

362. W.S. Cho, M. Yoshimura, *J. Am. Cer. Soc.*, 80 (1997) 2199

363. C. Burda, X. Chen, R. Narayanan, M.A. El-Sayed, *Chem. Rev.,* 105 (2005) 1025